biomedicines

MDPI

Article

PK2 Receptor Agonism Upregulates Astrocytic GDNF Expression to Promote Neuroprotection in Experimental Models of Parkinson's Disease

Jie Luo [1,†], Griffin Clabaugh [2,3,†], Matthew Neal [1], Bharathi N. Palanisamy [1], Minhong Huang [1], Souvarish Sarkar [1], Gary Zenitsky [2], Huajun Jin [2], Vellareddy Anantharam [2], Canan G. Nebigil [4], Laurent Désaubry [4], Arthi Kanthasamy [2] and Anumantha G. Kanthasamy [1,2,3,*]

[1] Department of Biomedical Sciences, Iowa State University, Ames, IA 50011, USA
[2] Isakson Center for Neurological Disease Research, Department of Physiology and Pharmacology, University of Georgia, Athens, GA 30602, USA
[3] Department of Biochemistry and Molecular Biology, University of Georgia, Athens, GA 30602, USA
[4] Regenerative Nanomedicine (UMR 1260), French National Institute of Health and Medical Research (INSERM), University of Strasbourg, Center of Research in Biomedicine of Strasbourg, 67084 Strasbourg, France; desaubry@unistra.fr (L.D.)
* Correspondence: anumantha.kanthasamy@uga.edu; Tel.: +1-706-542-2380
† These authors contributed equally to this work.

Abstract

Background/Objectives: Glial cell line-derived neurotrophic factor (GDNF) has demonstrated potent neuroprotective and neurorestorative effects in preclinical models of Parkinson's disease (PD). However, clinical trials using direct intracranial GDNF infusion or adeno-associated virus-mediated GDNF gene delivery have shown limited efficacy, in part because of challenges associated with invasive delivery. We previously identified prokineticin-2 (PK2) signaling as a compensatory protective pathway against dopaminergic neurodegeneration. This study investigated whether PK2 signaling regulates astrocytic GDNF expression and whether pharmacological activation of this pathway provides neuroprotection in PD models. **Methods:** Cultured astrocytes were treated with recombinant PK2 or the prokineticin receptor 1 (PKR1) agonist IS20, followed by assessment of GDNF gene expression and protein secretion. The neuroprotective effects of PK2/PKR1-mediated astrocytic signaling were evaluated in dopaminergic cell culture models. In male C57BL/6 mice and MitoPark transgenic mice, IS20 was administered systemically through intraperitoneal or intranasal routes, and brain GDNF levels and neuroprotective efficacy were evaluated in the MPTP-induced and chronically progressive MitoPark transgenic models of PD. **Results:** PK2 and IS20 significantly increased GDNF expression and secretion in cultured astrocytes and enhanced dopaminergic cell survival. Systemic administration of IS20 elevated GDNF levels in the mouse brain, including the nigrostriatal system. Moreover, IS20 treatment produced significant neuroprotective effects in both MPTP-treated mice and MitoPark transgenic mice. **Conclusions:** These findings identify PK2/PKR1 signaling as a novel regulator of astrocytic GDNF expression and support pharmacological activation of this pathway as a non-invasive strategy for enhancing endogenous GDNF signaling and protecting dopaminergic neurons in PD.

Keywords: Parkinson's disease; prokineticin-2; glial cell line-derived neurotrophic factor; IS20; astrocytes; neuroprotection

Received: 18 September 2026
Revised: 20 October 2026
Accepted: 27 October 2026
Published: 2 November 2026

Copyright: © 2026 by the authors. Licensee MDPI, Basel, Switzerland. This article is an open access article distributed under the terms and conditions of the Creative Commons Attribution (CC BY) license.

1. Introduction

As the second most common neurodegenerative disease, Parkinson's disease (PD) affects around 1% of the world's population aged ≥65 years. PD is mainly characterized by the progressive degeneration of dopaminergic (DAergic) neurons in the substantia nigra pars compacta (SNpc) in the ventral midbrain, resulting in dopamine depletion within the striatum. This neurodegeneration leads to hallmark motor symptoms, including bradykinesia, rigidity, and tremor [1,2]. Notably, autonomic and other non-motor deficits, such as sleep disturbances, anosmia, gastrointestinal dysfunction, and mood disorders, often precede the onset of motor symptoms, suggesting early involvement of extranigral brain regions in PD pathogenesis. The DA precursor, 3,4-dihydroxy-L-phenylalanine (L-DOPA), remains the standard-of-care treatment strategy, which temporarily alleviates motor symptoms by increasing brain DA levels. However, L-DOPA has limited efficacy in addressing motor symptoms and does not halt disease progression [3–5]. Since no disease-modifying therapies currently exist, the progressive nature of the disease typically demands dosage titration involving increasingly higher doses of L-DOPA, resulting in an array of motor fluctuations and other severe complications, including dyskinesia [2,6].

Glial cell line-derived neurotrophic factor (GDNF) is a well-characterized neurotrophic factor involved in the development and maintenance of multiple neuronal systems, including those of the kidney, enteric nervous system (ENS), and central nervous system (CNS) [7–10]. Since its discovery, GDNF has been recognized as one of the most potent neurotrophic agents, particularly within the DAergic system [11]. DAergic neurons express both the GDNF family receptor GFRα1 and the co-receptor RET, through which GDNF promotes neuronal survival, regeneration, and functional maintenance in the SN DAergic neurons. GDNF also increases DA content and uptake, stimulates neurite extension, and increases tyrosine hydroxylase (TH) expression in cell culture models [11,12]. In vivo evidence further supports that GDNF is necessary for the homeostatic maintenance of DAergic neurons during later stages of development and throughout adulthood. Supporting this, conditional knockout (cKO) of GDNF in mice starting at 2 mo old results in a selective decrease of TH immunoreactivity and a 60–70% loss of DA midbrain neurons by 9 mo of age, underscoring GDNF's indispensable role in DA neuron survival under physiological conditions [10]. Alternatively, another study reported that decreasing GDNF levels had minimal effect on survival of adult catecholaminergic neurons in vivo [13]. These divergent findings may be due to the different genetic models that were employed, such as the use of a Nestin-Cre deletion of the GDNF floxed allele occurring during development, allowing for potential embryonic compensation [14].

Numerous preclinical studies using rodent and non-human primate models of PD have demonstrated the therapeutic potential of GDNF [15–18]. However, early clinical trials administering recombinant (r)GDNF intracranially failed to uniformly diffuse into deeper layers of the brain and did not slow down neurodegeneration or improve motor function [13,19]. While improvements in GDNF delivery have yielded moderate efficacy [20], the major challenge of achieving long-term GDNF delivery into the brain remains. Additional safety concerns, including cerebellar toxicity, were also evident [21]. Gene therapy approaches using adeno-associated virus (AAV)-mediated GDNF gene delivery offered the potential to overcome the delivery limitations and were deemed safe in Phase I clinical trials. Nevertheless, Phase II trials failed to demonstrate therapeutic efficacy [22–24]. Moreover, AAV-mediated gene delivery is inherently less controllable than conventional pharmacotherapies due to its irreversible genomic integration, raising concerns about long-term safety and regulation [25]. Failures of current GDNF trials underscore the critical need to better understand upstream regulators of the GDNF signaling and to disentangle the complex network of pathways in crosstalk with GDNF. Targeting endogenous GDNF expression would represent a compelling neuropharmacological strategy and warrants increased translational research efforts [26,27].

Setbacks of current AAV-mediated DAergic GDNF gene-delivery trials have forced the rethinking of alternative strategies, including expressing GDNF specifically in striatal astrocytes. Astrocytes naturally secrete key neurotrophic factors NGF, BDNF, and GDNF [28], and are considered a primary source of GDNF in the brains of PD patients [29,30]. The role of astrocytes in maintaining a healthy environment for proper neuron function has been increasingly recognized, yet their potential as a source of nigral GDNF and as a viable therapeutic target remains underexplored. Harnessing astrocyte-mediated endogenous GDNF expression may offer a more physiologically relevant and controllable approach to neuroprotection in PD, warranting further investigation in deeper mechanistic and translational research.

Initially identified from a nontoxic component of black mamba snake venom [31], the prokineticin family proteins have been shown to interact with the GDNF signaling pathway in the peripheral nervous system (PNS) during development of the ENS [7,8,32,33]. Disruption of either signaling pathway is implicated in Hirschsprung disease, a rare congenital disorder of the ENS [34], highlighting the functional interdependence of GDNF and prokineticin signaling. This well-established crosstalk in the ENS raises the intriguing possibility that the prokineticin signaling pathway may also engage in similar crosstalk with GDNF in the CNS. Interestingly, both GDNF and prokineticin-2 (PK2) have been identified as potent chemoattractants for axons during neurogenesis/neuritogenesis. PK2, in particular, is essential for proper development of the olfactory bulbs (OB) [35]. Importantly, our previous work demonstrated that PK2 upregulation mediates a protective, compensatory response during neurodegeneration by activating the AKT and ERK pathways and enhancing mitochondrial biogenesis [36]. AAV2/5-mediated delivery of PK2 conferred neuroprotection against Parkinsonian toxicants in the SN and striatum [36]. Additional work from our lab revealed that PK2 promotes an anti-inflammatory, protective phenotype in astrocytes [37]. However, evidence is lacking for a fundamental relationship between PK2/PKR1 and GDNF/RET signaling in the CNS, particularly within the nigrostriatal system. Intriguingly, PKR1 is mainly expressed in astrocytes [38], raising the possibility that GDNF may be co-upregulated with the prokineticin pathway in astrocytes. The preferential expression of PKR1 over PKR2 in astrocytes further supports the therapeutic feasibility of selectively targeting astrocytes using PKR1-specific agonists. Based on this therapeutic rationale, using IS20, a lipophilic small-molecule receptor agonist specific to PKR1 [39], we hypothesized that positive modulation of the expression and secretion of GDNF in astrocytes of the nigrostriatal system could be achieved via pharmacological activation of PK2/PKR1 signaling. This astrocyte-derived trophic support may, in turn, promote DAergic neuronal survival and exert neuroprotective effects in experimental models of PD.

In this study, we report that (1) PK2/PKR1 signaling represents a novel and druggable pathway for modulating GDNF expression in the CNS, particularly in astrocytes, (2) the upregulation of GDNF through PK2/PKR1 signaling can be pharmacologically activated by intranasal (IN) or intraperitoneal (i.p.) delivery of the PKR1 receptor agonist IS20, and (3) IS20 could rescue DA neurons and their projections from degeneration in both genetic and chemically induced mouse models of PD. Unlike the uncontrolled, long-term continuous expression driven by intracerebral injections of GDNF viral vectors, which leads to unwanted compensatory responses [40–42], systemic administration of the small-molecule IS20 showed no such adverse effects, nor any overt toxicity (body weight, blood chemistries) in mice [39]. This distinction highlights the advantage of pharmacologically modulating endogenous GDNF expression in a more controlled and physiologically relevant manner. Thus, by pharmacologically modulating the magnitude and duration of endogenous GDNF expression using small-molecule IS20 treatment, GDNF's established clinical benefits could be fully harnessed while mitigating the risks associated with conventional gene-delivery approaches.

2. Materials and Methods

2.1. Calcium Assays

Intracellular calcium mobilization was assessed using the Fluo-4 NW Calcium Assay Kit (F36206, Thermo Fisher, Waltham, MA, USA) according to manufacturer's instructions. Briefly, CHO cells were grown on 96-well plates the previous day. FLIPR (Molecular Devices, San Jose, CA, USA) was used to inject dissolved IS20 into the cell plate wells, which were read on a FlexStation multi-mode microplate reader (Molecular Devices).

2.2. Animal Handling

All mice were housed under a 12-h light cycle in a climate-controlled mouse facility (22 ± 1 °C) with food and water available ad libitum. The individual mouse served as the experimental unit for all in vivo experiments. Male C57BL/6 mice were pre-screened during behavior assessments for normal baseline performance before being randomly assigned to experimental groups. Animals showing wounds or abnormal behaviors were to be excluded from the study; no animals met these exclusion criteria, and no animals were excluded from the analyses. Investigators involved with data collection and analysis were not blinded to group allocation.

2.3. MPTP Injections

Over a 5-day period, one i.p. injection of 20 mg/kg MPTP was administered every day to each mouse in the MPTP group, and an equal volume of saline (vehicle) was similarly injected into each mouse in the control group.

2.4. Behavior Monitoring

All groups were monitored for voluntary, exploratory locomotor activity using the automated VersaMax analyzer (model VMAUSB, AccuScan, Columbus, OH, USA) connected to a VersaMax motion-detection monitor (model RXYZCM-16). The 40 × 40-cm square monitor was partitioned into four, 20 × 20-cm square open-field arenas. The VersaMax system is capable of tracking two animals simultaneously when using two diagonally opposed arenas that did not share a wall of infrared (IR) beams. Each animal was allowed to acclimate to its arena for 2 min, after which its spontaneous locomotor activities (horizontal activity, vertical activity, and speed), monitored as IR beam-breaks, were recorded for 10 min. Fusion software 6.2 was used to generate heat maps (Omnitech Electronics, Columbus, OH, USA).

The Rotarod assessment was performed to measure coordination and balance using a Rotarod apparatus (Harvard Apparatus, Holliston, MA, USA) as previously described [43–45]. The mice were acclimatized to the test room for 1 h prior to assessment. The constant acceleration mode was used to test coordination and balance performance starting at 2 RPM and ramping up to 40 RPM across a 5-min testing period. The time spent on the rotating rod was measured as the latency to fall. Three trials were performed per day for four consecutive days, with the first three days being training days and the fourth as the test day.

To assess olfactory function, we utilized the social discrimination test as previously described [43,44]. Each mouse was placed in a chamber and received bedding from its own cage on one side and bedding from a cage housing four opposite-sex mice that had been changed one week prior to collection on the other side. Using the ANY-maze tracking software (v6.2; Stoelting, Wood Dale, IL, USA), we measured the time spent sniffing the defined zone surrounding the bedding by tracking the animal's head. The total number of bouts of sniffing each defined zone was measured during a 3-min interval.

2.5. MitoPark Mouse Model of PD

MitoPark mice were a kind gift from Dr Nils-Göran Larsson of the Karolinska Institute, Stockholm, Sweden, from his laboratory at the Max Planck Institute for Biology of Ageing. The MitoPark Tg mouse model is created by mitochondrial transcription factor A (TFAM) inactivation specifically in DA neurons by cKO through control of the DA transporter promoter. The mice used were from our MitoPark breeding colony at Iowa State University. After behavioral experiments were performed at the predetermined ages, mice were euthanized at the predetermined endpoints via CO_2 asphyxiation, as outlined in approved IACUC protocols, and samples were processed for either RT-qPCR or Western blotting.

2.6. Western Blot

Dissected brain regions were collected in Eppendorf tubes and flash-frozen. To isolate total protein, RIPA buffer containing sodium orthovanadate and Protease and Phosphatase Inhibitor Cocktail (Thermo Fisher 78440) was added to each tube and homogenized using a tissue homogenizer. Dissolved total lysate was centrifuged at 12,000× *g* for 60 min to remove cellular debris. Normalized protein samples were loaded into each well of a 12-well plate and were separated by sodium dodecyl sulfate (SDS) gel electrophoresis (100 V, 90 min), using Any kD Mini-PROTEAN resolving gel (4569035, Bio-Rad, Hercules, CA, USA). Proteins on SDS gels were then transferred to a nitrocellulose membrane (26 V, overnight) and blocked for 1 h using fluorescent Western blocking buffer (Rockland Immunochemicals, Pottstown, PA, USA). Primary antibodies diluted in blocking buffer with 0.05% Tween 20 were then added to the membranes and incubated overnight at 4 °C. Primary antibodies were diluted as follows: rabbit anti-TH (1:1000; Millipore, Burlington, MA, USA, Cat# AB152), rabbit anti-PK2 (1:500; Novus Biologicals, Centennial, CO, USA, Cat# NBP2-94101), goat anti-GDNF (1:500; Santa Cruz Biotechnology, Dallas, TX, USA, Cat# sc-328), goat anti-IBA1 (1:1000; Abcam, Waltham, MA, USA, Cat# ab5076), rabbit anti-AKT (1:500; Cell Signaling Technology, Danvers, MA, USA, Cat# 4691), rabbit anti-pAKT (Ser473) (1:500; Cell Signaling, Cat# 4060) and rabbit anti-PKR1 (1:500; Alomone, Jerusalem, Israel, Cat# APR-041). The next day, primary antibodies were removed, and blots were washed (7 times, 5 min each) in PBS wash buffer containing 0.05% Tween 20 (PBST).

Secondary antibody (infrared dye-tagged) was added for 1 h. Blots were then triple-washed in PBST and once in PBS. The protein β-actin was used as a loading control. Membranes were scanned using the Odyssey IR imaging system (LI-COR, Lincoln, NE, USA) and digital images were captured via a LI-COR Odyssey imager. Densitometric analysis was done using ImageJ software v2.7.0.

2.7. IHC

Cells were fixed in 4% paraformaldehyde, blocked with BSA and Triton-X to permeabilize the cell membranes. Primary antibodies were diluted as follows: rabbit anti-TH (1:1600; Millipore, Cat# AB152), anti-GDNF (1:500; Santa Cruz D20, Cat# sc-328), and rabbit anti-PKR1 (1:500; Alomone, Cat# APR-041). Alexa Fluor fluorescent secondary antibodies (Thermo Fisher) were used against primary antibodies for fluorescent imaging. For DAB staining, HRP-conjugated secondary antibodies were used against primary antibodies, and VECTASTAIN Elite ABC HRP Kit (Vector Labs, Newark, CA, USA) was used for conjugating HRP to secondary antibodies. DAB was used for colorimetric detection.

2.8. SYBR Green RT-qPCR

To obtain total RNA, tissue lysis buffer from the Absolutely RNA Miniprep kit (Agilent Technologies) was added to dissected, region-specific brain tissue samples together with beta-mercaptoethanol as a reducing agent to preserve RNA. A tissue homogenizer was used to dissolve tissue into the lysis buffer, and lysates were processed according to the kit manufacturer's instructions. Total RNA isolated from each sample was quantified using NanoDrop (Thermo Scientific) to determine RNA concentration and purity. First, strand cDNA synthesis was performed using the Affinity Script qPCR cDNA synthesis system (Agilent Technologies) with 1 μg of total RNA in the reaction mixture. Real-time PCR was performed with the RT² SYBR Green master mix (Qiagen, Germantown, MD, USA) using diluted cDNA and QuantiTect (Qiagen) mouse primer sets. The 18S rRNA gene (mouse) was used as the housekeeping gene to normalize each sample. The amount of each template was optimized empirically to maximize efficiency without inhibiting the PCR reaction. After the last cycle of the qPCR run, dissociation curves were run to ensure a single amplicon peak was obtained, indicating primer specificity. The results are reported as fold change in gene expression derived with the $\Delta\Delta C_t$ method, using the threshold cycle (C_t) value for the housekeeping gene and for the respective gene of interest in each sample. Control animals serve as the baseline for fold change.

2.9. HPLC Analysis of Striatal DA Levels

HPLC samples were processed as previously described [36] (Gordon et al., 2016). Briefly, mice were euthanized, striata were collected, and neurotransmitters were extracted in 0.2 M perchloric acid solution containing 0.05% Na_2EDTA, 0.1% $Na_2S_2O_5$ and isoproterenol (internal standard). DA and metabolites were separated isocratically by a reversed-phase column with a flow rate of 0.6 mL min^{-1} using a Dionex Ultimate 3000 HPLC system (pump model ISO-3100SD, Thermo Scientific) equipped with a refrigerated automatic sampler (model WPS-3000TSL). The CoulArray (model 5600A) electrochemical detection system was coupled with an analytical cell (microdialysis cell model 5014B) and a guard cell (model 5020). Data acquisition and analysis were performed using Chromeleon 7 and ESA CoulArray 3.10 HPLC Software.

2.10. Cell Culture

To generate primary mouse culture, astrocytes were obtained from the whole brain homogenate of 0- to 3-day-old mouse pups. Astrocytes were collected, isolated, and maintained as previously described [37] by utilizing DMEM media (10% heat-inactivated FBS, 100 U/mL penicillin, 100 μg/mL streptomycin, and 2 mM glutamate) to grow the cells. Human U373 astrocytoma cells (ATCC) were grown according to ATCC instructions in MEM media supplemented with 10% FBS, penicillin (100 U/mL) and streptomycin (100 μg/mL). Human astrocytes were obtained from Lonza (Allendale, NJ, USA) and grown according to company instructions in astrocyte growth media (AGM, CC-3186). All cells were maintained in an incubator at 37 °C with 5% CO_2.

2.11. CRISPR/Cas9-Based Knockdown of PKR1 in U373 Cells

The lentivirus-based CRISPR/Cas9-mediated knockdown (KD) of PKR1 was performed as previously described [37]. The pLV-U6gRNA-Ef1aPuroCas9GFP-PKR1 plasmid, containing a PKR1-targeting gRNA directed against exon 2, was purchased from Sigma-Aldrich (St. Louis, MO, USA). To generate the PKR1 CRISPR and control lentivirus, the lenti-CRISPR/Cas9 PKR1 KD plasmid and control plasmid were transfected into 293FT cells with the Mission Lentiviral Packaging Mix from Sigma-Aldrich according to the company's protocol. The lentivirus was harvested 48 h post transfection, and titers were measured using the Lenti-X p24 Rapid Titer Kit (Clontech, Mountain View, CA, USA). For

stable knockdown of PKR1 in U373 cells, cells were grown in six-well plates with a seeding density of 0.1×10^6 cells per well in growth media, and lentivirus was added to the media at an MOI of 100 and incubated for 24 h. After 24 h, fresh media supplemented with puromycin (50 μg/mL) was added to the cells for stable cell selection.

2.12. Mitochondrial Dynamics Analysis

To measure mitochondrial dynamics, a Seahorse XFe24 Analyzer (Agilent Technologies, Santa Clara, CA, USA) was used to measure mitochondrial oxygen consumption rates with the Mito Stress Test. The calibration plate was hydrated overnight in a non-CO_2 incubator. The treatments were done in serum-free medium. We used 0.75 μM oligomycin, 1 μM FCCP, and 0.5 μM rotenone/antimycin for the Mito Stress Test. The Mito Stress Report Generator was used for analysis.

2.13. MTS Assay

Cells were plated in 96-well plates. After treatment, 10 μL of MTS dye (Promega, Madison, WI, USA) incubated for 1.5 h in each well. Following incubation, a plate reader was used to take excitation and background (subtracted) readings at 490 and 660 nm, respectively.

2.14. Human Samples

Human PD and age-matched control patient SN tissues were obtained from the Miami Brain Endowment Bank at the University of Miami (Miami, FL, USA) as previously described [46]. The control patient ages were 80 ± 7.85 years, and the PD patient ages were 82 ± 7.65 years.

2.15. Data Analysis

All in vitro data were determined from at least two biologically independent experiments, each done with a minimum of three biological replicates. Data analysis used Prism 10.5.0 software (GraphPad Software, San Diego, CA, USA) to perform one-way ANOVA and then Bonferroni's post-hoc test or two-way ANOVA to compare all treatment groups. Student's *t*-test (two-tailed) was used when two groups were being compared. Differences with $p \leq 0.05$ were considered statistically significant.

3. Results

3.1. Prokineticin Receptor 1 (PKR1) Is Activated by rPK2 Protein and by the Receptor Agonist IS20

Previous work in our lab has demonstrated that PK2 signaling functions as a potent neuroprotective response during early stages of DAergic neurodegeneration in models of PD and promotes a protective, anti-inflammatory phenotype in astrocytes [36,37]. Given the established crosstalk between prokineticin signaling and GDNF during development, and the well-characterized protective effect of GDNF in preclinical models of PD, we hypothesized that PK2's neuroprotective functionalities may occur, in part, through activation of GDNF signaling. PKR1 is expressed on the membrane of DAergic neurons and Type 1 astrocytes in the nigrostriatal system. We confirmed PKR1 and GDNF expression in the SN by immunostaining human postmortem nigral sections (Supplementary Figure S1a). Interestingly, we found that PKR1 is highly expressed in the SN and colocalized with GDNF, indicating the possibility of GDNF expression being downstream of PKR1 signaling. We also found a marked decrease in GDNF mRNA levels (Supplementary Figure S1b) in PD patient nigral lysates compared to control, consistent with some previous reports [30,47] while conflicting with others [48]. This decrease in GDNF highlights the lack of trophic support in the nigrostriatal system in PD patients and the therapeutic potential of restoring GDNF levels in the SN.

To examine whether the PK2 agonist IS20 can positively modulate GDNF expression, our initial set of experiments was conducted to confirm that IS20 activates PKR1 as previously reported [39,49]. Once activated, PKR1 initiates downstream signaling that culminates in the rise in Ca^{2+} in the cytosol [39,50]. In silico modeling with AlphaFold3 of PK2 binding to PKR1 confirmed that the AVITGA sequence motif resides in the binding pocket of PKR1 (Supplementary Figure S2a). This is in alignment with previous reports of AVITGA being required for receptor binding. In silico analysis also revealed that IS20 can bind PKR1 with high affinity (Supplementary Figure S2b).

To experimentally examine PKR1 activation, we used a CHO cell line stably expressing PKR1. The PKR1-overexpressing cells were treated with 100 nM rPK2 or 10 μM IS20, and PKR1 activation was monitored by measuring intracellular Ca^{2+} mobilization in real time over 180 s using a Fluo-4 NW calcium assay kit. Upon treatment with rPK2, intracellular Ca^{2+} concentration rose rapidly, peaking at 20 s post-treatment (Supplementary Figure S2c), indicative of a Gαq1-mediated mechanism for PKR1 activation. Treatment with 10 μM of IS20 caused Ca^{2+} concentration to rise more slowly, peaking at 180 s post-treatment (Supplementary Figure S2d), suggesting that IS20 induces a similarly large but relatively delayed activation of PKR1 compared to rPK2.

3.2. Activation of PKR1 by Recombinant PK2 or the PK2 Agonist IS20 Upregulates GDNF Expression in Human Astrocytes

To examine the effects of PK2 signaling activation on GDNF expression in astrocytes, we first incubated U373 human astrocyte cells with rPK2 protein dissolved in reduced serum (2% FBS). Treatment with 25 nM rPK2 for 8 h induced GDNF mRNA expression levels to nearly 2.5-fold above vehicle control (Figure 1a), and a 10-h treatment induced GDNF protein levels by ~1.7-fold (Figure 1b). The rPK2-induced upregulation of GDNF mRNA was completely attenuated by co-treatment with the PKR1 selective antagonist PC-7 (Figure 1a). To validate these findings in primary human cells, primary human astrocytes were incubated with 25 nM rPK2 for 10 h and analyzed with immunocytochemistry (ICC). Indeed, we observed a significant increase in GDNF signal in rPK2-treated astrocytes (Figure 1c).

Next, we sought to determine if IS20 pharmacological activation of PKR1 could modulate GDNF in human U373 astrocytes. A time-course treatment of U373 cells with 10 μM IS20 revealed a 3-fold increase in GDNF mRNA after 1 h of IS20 incubation; this upregulation gradually declined over the subsequent 5 h (Figure 1d). To assess any receptor-specific effects of IS20 on GDNF production, we overexpressed PKR1 by transiently transfecting increasing amounts of PKR1 expression vector into U373 astrocytes. Ectopic expression of PKR1 (0.5–5 μg cDNA) dose-dependently stimulated the upregulation of GDNF mRNA in cells treated with 10 μM IS20 for 4 h (Figure 1e). Conversely, when a CRISPR-Cas9 guide RNA against PKR1 was used to knock down PKR1 in U373 astrocytes (Figure 1f), IS20 was no longer able to modulate GDNF expression (Figure 1g), further demonstrating that IS20-induced GDNF expression is highly dependent on PKR1 receptor binding and activation.

To further determine whether IS20 enhances GDNF expression by increasing GDNF promoter activity, we utilized a GDNF promoter luciferase assay. U373 astrocytes were transfected with a 3.6-kb GDNF promoter fragment that encompasses GDNF promoter 1, TATA-box, the main transcriptional start site and exon 1 of the murine GDNF gene cloned into a pGL3 promoter vector that drives the expression of a luciferase reporter gene. After 24 h of transfection, U373 cells were treated with 5 μM and 10 μM of IS20 for 8 h. We observed a dose-dependent increase in luciferase signal intensity with both doses significantly enhancing GDNF promoter activity (Figure 1h). Next, we treated the transfected U373 cells with IS20 (10 μM) for 4 and 8 h (Figure 1i,j). IS20 significantly increased relative luciferase activity at all time points. Co-treatment with the PK2 receptor antagonist PKRA7 attenuated IS20-induced promoter activation in 4 and 8 h groups (Figure 1i,j).

Together, these results suggest that IS20 can enhance GDNF promoter activity and gene expression in U373 astrocytes.

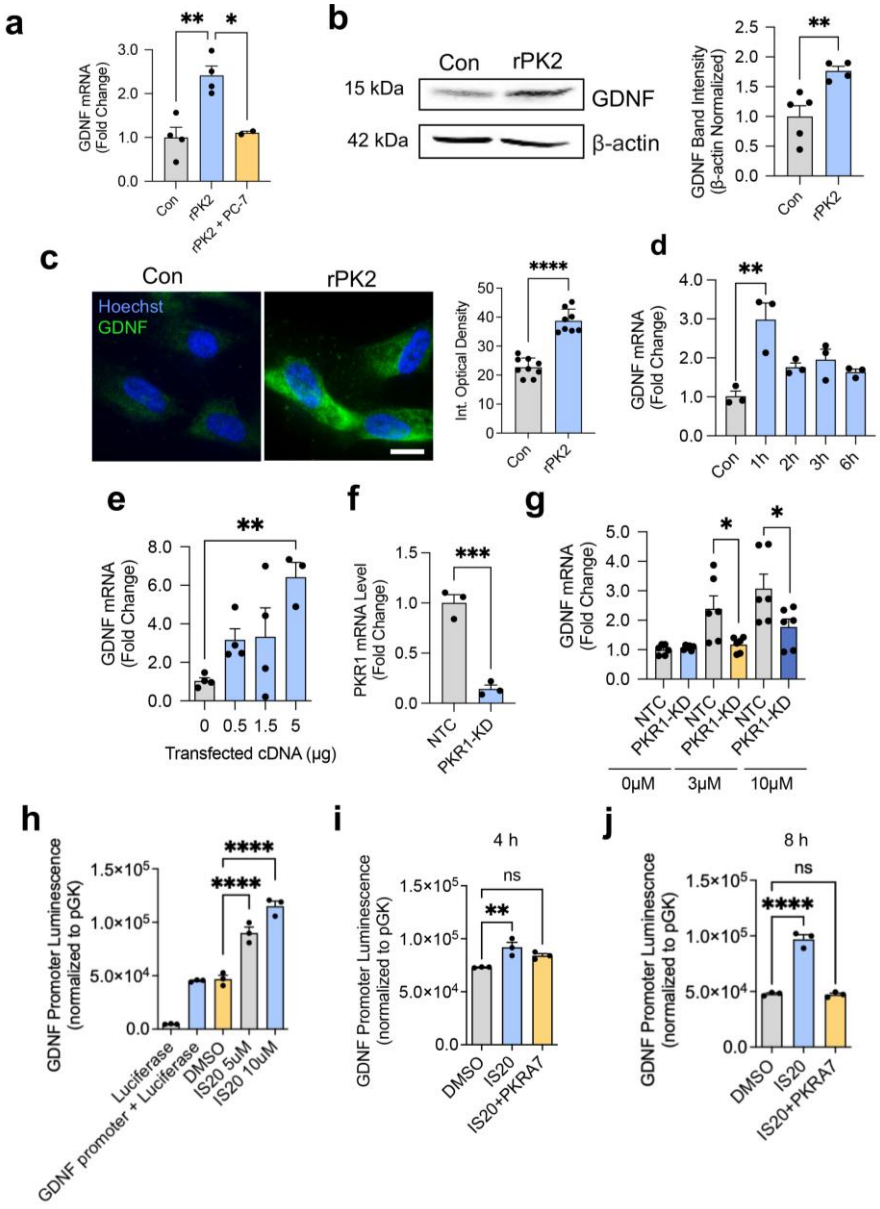


Figure 1. Recombinant PK2 (rPK2) and the PKR1 agonist IS20 induce GDNF expression in human astrocytes. (**a**) RT-qPCR of GDNF mRNA expression in U373 human astroglioma cell line treated with rPK2 (25 nM) for 8 h, with or without co-treatment using the PKR1 inhibitor PC-7 (1 μM) (n = 4). (**b**) Western blot analysis and densitometric quantification of GDNF levels in U373 cells treated with rPK2 (25 nM) for 10 h (n = 4). (**c**) Immunocytochemical analysis and quantification of GDNF in primary human astrocytes treated with 25 nM rPK2 for 10 h (n = 8; scale bar = 10 μm). (**d**) RT-qPCR analysis of GDNF gene expression of U373 cells treated with IS20 (10 μM) for 1–6 h (n = 3). (**e**) GDNF mRNA levels measured by RT-qPCR of U373 astrocytes transiently transfected with a PKR1 over-expression vector with increasing amounts of cDNA (0.5–5 μg) and treated with 10 μM IS20 for 4 h (n = 3–4). (**f**) RT-qPCR analysis of PKR1 mRNA confirming CRISPR-Cas9 PKR1-KD. (**g**) RT-qPCR analysis of GDNF mRNA in CRISPR-Cas9 PKR1-KD cells treated with IS20 (3–10 μM) for 8 h (n = 6). (**h**) GDNF promoter-driven luminescence activity in U373 astrocytes transfected with a 3.6-kb GDNF promoter fragment and treated with IS20 (5 μM or 10 μM) for 8 h. (**i**) GDNF promoter luciferase activity following 4 h and (**j**) 8 h of 10 μM IS20 or co-treatment of IS20 and PKRA7 (2 μM) in U373 astrocytes following promoter transfection. * $p \leq 0.05$, ** $p < 0.01$, *** $p < 0.001$, **** $p < 0.0001$.

3.3. GDNF Is Upregulated in Primary Mouse Astrocytes and Organotypic Midbrain Slice Cultures Treated with rPK2 and IS20

Next, we used cultured primary mouse astrocytes from prenatal mouse pups to validate the findings obtained from human astrocyte cells. Treating primary mouse astrocytes with rPK2 (10–25 nM) for 8 h produced a 3.4-fold upregulation of GDNF mRNA in the 25-nM group, which was abolished with PC-7 antagonism (Figure 2a). Western blot confirmed a corresponding increase in GDNF protein levels (Figure 2b).

Before assessing IS20 responsiveness, we evaluated the potential toxicity of IS20 on primary mouse astrocyte survival using an MTS assay. We found the 24-h LD50 for IS20 ranged between 348 μM and 592 μM IS20 (Supplementary Figure S3a), indicating a wide therapeutic window for the 10 μM IS20 concentration used in subsequent experiments. To assess the GDNF response to IS20, we treated primary mouse astrocytes with 10 μM IS20 for 1–2 h. We found that IS20 induced a rapid upregulation of GDNF mRNA (Figure 2c), accompanied by increased GDNF protein secretion into the culture media as measured by ELISA (Figure 2d). A dose–response study (0.5–30 μM IS20 for 2 h) further identified 10 μM as the optimal dose in primary mouse astrocyte cells to elicit maximal GDNF induction and secretion (Figure 2e,f). Interestingly, mRNA levels of the predominant GDNF receptor in the DAergic system, GFRα1, were co-upregulated with GDNF following 10 μM IS20 treatment (Supplementary Figure S3b), indicating that the increased gene expression and protein secretion of GDNF also lead to upregulated ligand–receptor interaction, possibly through a positive feedback loop, to promote GDNF signaling. GDNF protein levels were also increased in whole-cell lysates treated with 1 and 10 μM of IS20 for 4–8 h (Figure 2g). Moreover, ICC analysis confirmed increased GDNF following 8 h of 10 μM IS20, further demonstrating that GDNF is both upregulated and secreted by primary astrocyte cells following IS20 treatment (Figure 2h).

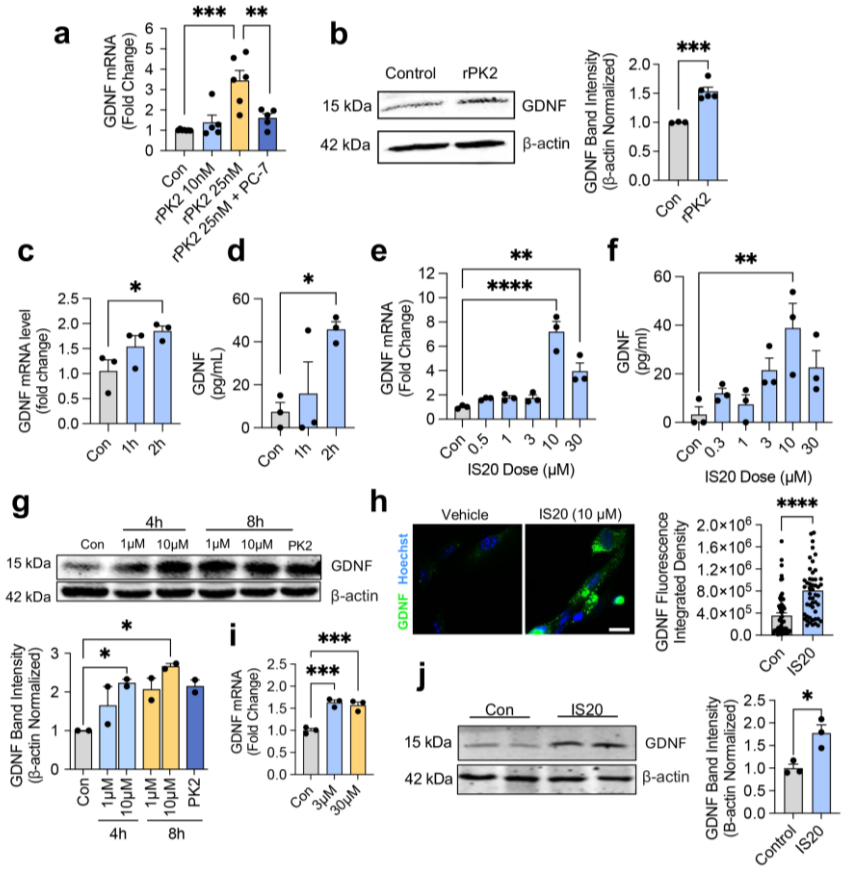


Figure 2. rPK2 and IS20 increase GDNF expression in primary cultures of mouse astrocytes and organotypic slices. (**a**) RT-qPCR analysis of GDNF mRNA in primary mouse astrocytes treated with

rPK2 (10–25 nM), with or without co-treatment with PC-7 (1 μM) for 8 h ($n = 6$). (**b**) Western blot analysis and quantification of GDNF levels in primary mouse astrocytes treated with rPK2 (25 nM) for 10 h ($n = 3$–5). (**c**) RT-qPCR assay of GDNF mRNA in primary mouse astrocytes treated with 10 μM IS20 for 1–2 h ($n = 3$). (**d**) GDNF ELISA of the supernatant of primary mouse astrocytes treated with 10 μM IS20 for 1–2 h ($n = 3$). (**e**) RT-qPCR analysis of GDNF mRNA of primary mouse astrocytes treated with 0.5–30 μM IS20 for 3 h ($n = 3$). (**f**) GDNF ELISA of the supernatant of primary mouse astrocytes treated with 0.3–30 μM IS20 for 2 h ($n = 3$). (**g**) Western blot analysis of GDNF levels (left) in primary astrocyte lysates treated with 1 μM or 10 μM IS20 or 25 nM PK2 for 4 h or 8 h and densitometric analysis (right) of the GDNF band normalized to β-actin ($n = 2$). (**h**) GDNF immunocytochemistry of primary human astrocytes treated with IS20 (10 μM) for 8 h ($n = 4$, scale bar = 10 μm). (**i**) RT-qPCR analysis of GDNF gene expression in cultured midbrain organotypic slices treated with 0, 3, or 30 μM IS20 for 4 h ($n = 3$). (**j**) Western blot analysis and quantification of GDNF protein levels in cultured organotypic slices treated with 0 or 30 μM of IS20 for 4 h ($n = 3$). * $p \leq 0.05$, ** $p < 0.01$, *** $p < 0.001$, **** $p < 0.0001$.

To further evaluate the specificity of IS20 in stimulating GDNF expression, we used IS21, an analog of IS20 incapable of activating PKR1. Treating primary mouse astrocytes with IS21 for 3 h did not confer GDNF expression, while IS20 induced a 3-fold increase in GDNF mRNA (Supplementary Figure S3c,d). Moreover, using Qiagen Neurotrophin and Receptor PCR array analysis, we found increased expression of 71 out of 84 genes in primary mouse glial cultures treated with IS20, including GDNF, CNTF, and NTF3 (Supplementary Figure S3e), further supporting the idea that IS20 can promote neurotrophic support in astrocytes.

After establishing IS20's effects on GDNF expression using astrocyte cultures, we validated those findings using an ex vivo approach employing organotypic midbrain slice cultures prepared from neonatal mouse pups. In line with our in vitro findings, treating organotypic midbrain slices with IS20 for 4 h increased GDNF mRNA expression (Figure 2i) and protein levels (Figure 2j). Collectively, these results demonstrate that GDNF is highly upregulated and secreted in both primary mouse astrocyte and midbrain slice cultures following PK2 and IS20 activation of PKR1 signaling.

3.4. IS20 Protects Against MPP⁺-Induced Cell Death and Preserves Mitochondrial Energetics in DAergic Neuronal Cells

Having established IS20 as a potent inducer of GDNF in astrocytes, we further evaluated whether IS20-induced astrocytic GDNF upregulation and secretion could functionally protect DAergic neuronal cells from the classic Parkinsonian toxicant MPP^+. U373 astrocytes were incubated with or without IS20 for 2 h, followed by a change to fresh media and an additional incubation for 6 h. Astrocyte-conditioned media (ACM) from both groups were collected and added to N27 DAergic neuronal cells that were then co-treated with or without MPP^+ (100–300 μM) for 24 h (Figure 3a). IS20-treated ACM significantly increased cell viability in MPP^+-treated N27 cells compared to MPP^+-treated cells that had received only vehicle-treated ACM (Figure 3b). Next, we investigated whether this protection was mediated through preservation of mitochondrial respiration. Seahorse analysis revealed that, in addition to slightly increasing the basal respiration of untreated N27 cells (Figure 3c), IS20-treated ACM remarkably attenuated the MPP^+-induced reduction in basal respiration, maximum respiratory capacity, and reserve capacity (Figure 3d–f), suggesting that a mitochondrial mechanism at least partly contributes to the protection conferred by IS20-treated ACM. Lastly, we utilized mouse primary mesencephalic culture to validate the neuroprotective effects of IS20-treated ACM. We included the ACM collected from U373 astrocytes treated with IS21, an analog of IS20 that does not activate PKR1, to further determine the specificity of IS20. IS20-treated, but not IS21-treated, ACM promoted cell survival in MPP^+-exposed mouse primary mesencephalic culture as determined by MTS assay (Figure 3g). Altogether, these studies suggest that IS20-treated

astrocytes secrete protective factors, likely including GDNF, that protect DAergic neuronal cells against MPP⁺-induced neurotoxicity and preserve mitochondrial energetics.

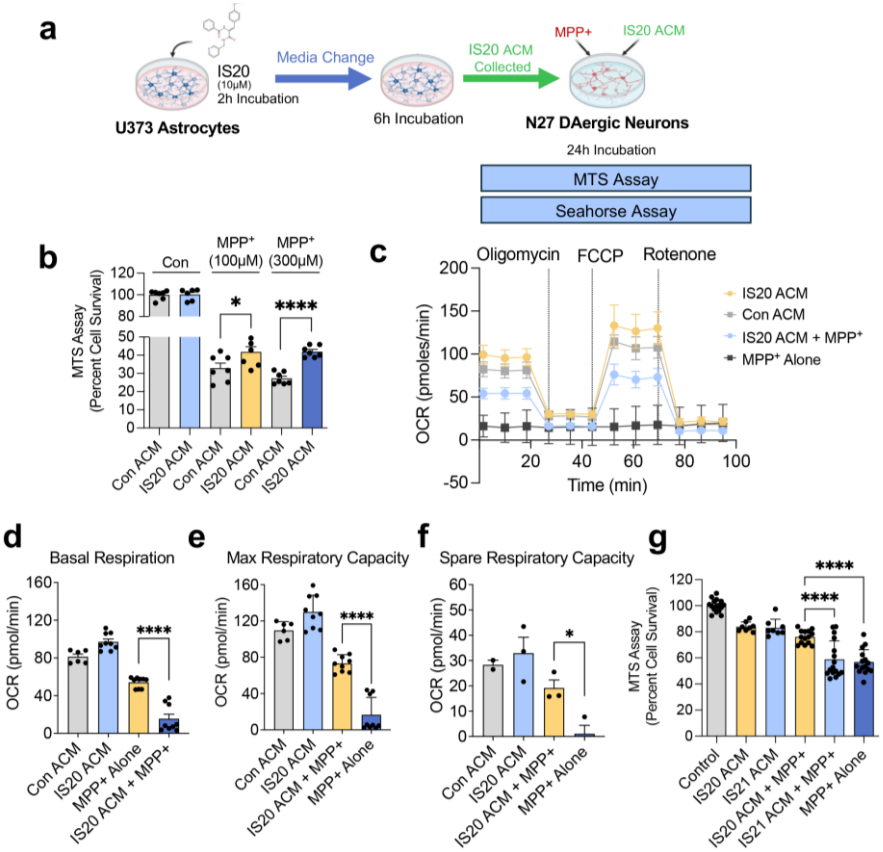


Figure 3. IS20 protects against MPP⁺-induced cell death and preserves mitochondrial energetics in DAergic neuronal cells. (**a**) Schematic of the IS20 treatment paradigm whereby U373 astrocytes were treated with 10 μM IS20 or vehicle control for 2 h, the media was changed and the U373 astrocyte cells were incubated for 6 h. Next, the astrocyte media was collected and added to N27 DAergic neuronal cells that were co-treated with or without MPP⁺ (100 μM or 300 μM). Figure generated using BioRender. (**b**) MTS assay of N27 DAergic neurons after co-treatment with MPP⁺ and astrocyte-conditioned media (ACM) that had been incubated with or without IS20 for 24 h (n = 6–7). (**c**) Seahorse Mito Stress Test of N27 cells treated with control ACM (grey line), IS20 ACM (yellow line), IS20 ACM added with MPP⁺ (blue line), and MPP⁺ alone (black line) (n = 4 replicates). (**d**–**f**) Basal respiration, maximum respiratory capacity, and spare respiratory capacity as evaluated by the Seahorse Mito Stress Test. Student's t-test was used to assess difference between IS20-ACM + MPP⁺ and MPP⁺ Alone. (**g**) MTS assay of primary striatal culture isolated from the mouse and treated with the same control ACM, control ACM with MPP⁺, IS20 ACM + MPP⁺, IS21 ACM + MPP⁺, and the controls. * $p \leq 0.05$, **** $p < 0.0001$.

3.5. IS20 Administration Induces GDNF Expression and Release in C57BL/6 Mice

Next, we determined the bioavailability of IS20 in the brain after i.p. injection or IN administration and assessed its biological effects on endogenous GDNF expression. Wild-type C57BL/6 mice (8–12-wk-old males) were first i.p.-injected with IS20 (10 mg/kg body weight) or vehicle (DMSO). This dose was chosen based on the previous literature, which established effective cardioprotective outcomes by administering IS20 at 1 mg/kg via i.p. [49]. Considering that the blood–brain barrier substantially reduces CNS bioavailability after systemic administration, we utilized a higher dose of 10 mg/kg to overcome this, while still remaining well below the reported median lethal dose of 900 mg/kg and the lowest effective dose of in vivo toxicity of 170 mg/kg. [49] Eight hours after injecting mice

with IS20, GDNF levels were elevated in the SN and serum as assessed by Western blot and ELISA, respectively (Figure 4a,b). We next tested the IN route, which is known to concentrate small lipophilic compounds more efficiently in the brain than i.p. injections [51,52]. This is likely because the olfactory and trigeminal nerve pathways allow IN-administered compounds to bypass the blood–brain barrier, thus increasing compound bioavailability in the CNS noninvasively while reducing exposure to peripheral tissues [51,52]. Anticipating improved CNS bioavailability, we opted for a lower IN dose of 3 mg/kg IS20. Pharmacokinetic analysis using liquid chromatography/mass-spectrometry (LC/MS) revealed that IN-injected IS20 reached 4 ng/mg tissue in the whole brain at 30 min post-delivery, gradually decreasing to 1.5 ng/mg at 90 min and <0.8 ng/mg at 6 h (Supplementary Figure S4a), indicating that IN-injected IS20 was able to cross the blood–brain barrier and accumulate in the brain. Interestingly, the brain level of IS20 remained relatively high even 24 h post-IS20 treatment. ELISA detected concurrent increases in GDNF protein in both brain lysates and serum (Figure 4c,d), with both responses peaking at 30 min post-IS20 treatment. Similar to i.p. injections of IS20, at 3 and 6 h post-IN administration, RT-qPCR assays showed significant increases in GDNF mRNA in the SN and striatum (Figure 4e). GDNF mediates pro-survival effects through its preferred receptor GFRα1, a glycosylphosphatidylinositol (GPI) protein, and its co-receptor RET, a receptor tyrosine kinase that transduces intracellular signals and whose decreased expression causes progressive degeneration of the nigrostriatal system [24,53]. Intriguingly, IS20 significantly increased the expression of GFRα1 and RET mRNAs in whole brain lysates (Figure 4f,g). Collectively, these data show that both minimally invasive i.p. delivery and noninvasive IN delivery of IS20 effectively upregulate GDNF and its receptors in the mouse brain, supporting IS20 as a feasible therapeutic strategy for modulating endogenous neurotrophic support in vivo.

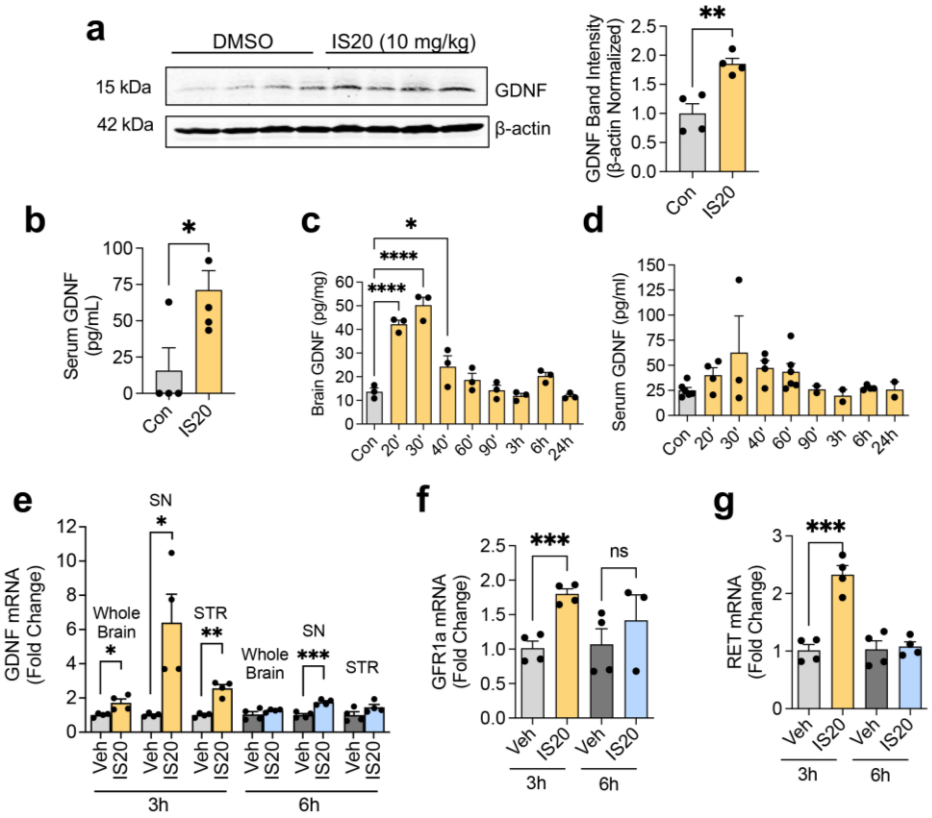


Figure 4. Intraperitoneal or intranasal administration of IS20 induces GDNF family neurotrophic factors in wild-type C57BL mice. (**a**) Western blot analysis probing for GDNF in substantia nigra (SN) lysates from mice intraperitoneally injected with 10 mg/kg IS20 8 h post-administration. (**b**)

GDNF ELISA of blood serum 8 h after sacrifice of 10 mg/kg IS20-treated and vehicle-treated mice. (**c**,**d**) ELISA assay of GDNF protein between 20 min and 24 h post intranasal IS20 (3 mg/kg) administration as measured in the (**c**) brain and (**d**) blood serum. (**e**) GDNF RT-qPCR of the whole brain, SN, and striatum (STR) 3 h and 6 h after intranasal treatment with IS20 (3 mg/kg). (**f**,**g**) RT-qPCR analysis of whole brain lysates collected 3 and 6 h post intranasal IS20 (3 mg/kg) administration, showing fold change in mRNA expression of (**f**) GFRa1 and (**g**) RET. * $p \leq 0.05$, ** $p < 0.01$, *** $p < 0.001$, **** $p < 0.0001$.

3.6. IS20 Protects Against 1-Methyl-4-phenyl-1,2,3,6-tetrahydropyridine (MPTP)-Induced GDNF and DA Metabolite Reductions in C57BL/6 Mice

Since intracranial delivery of exogenous rGDNF has shown effective neuroprotection [54], we hypothesized that the early IS20-mediated induction of striatal GDNF would preserve DA metabolite levels in a mouse model of PD. To test this, we co-injected C57BL/6 mice (8–12-wk-old males) with the classic Parkinsonian toxicant MPTP and IS20 i.p. once daily for 5 d, with IS20 being injected 1 h after MPTP. Mice then received IS20 alone for another 7 d (Figure 5a). This intervention strategy of combining co-treatments and a post-insult paradigm allowed us to examine IS20's effect on the early neurodegenerative process. As confirmed by RT-qPCR, MPTP treatment alone moderately reduced striatal GDNF gene expression, while IS20 co-treatment significantly preserved GDNF gene expression in MPTP-treated mice (Figure 5b). In concordance with our above-mentioned in vitro, ex vivo, and in vivo pharmacodynamics experiments, the largest fold change in GDNF gene upregulation occurred in mice treated with IS20 alone (Figure 5b). HPLC analysis of striatal homogenates showed that IS20 treatment modestly but significantly attenuated the MPTP-induced depletion of DA and its metabolites HVA and DOPAC (Figure 5c–e). These results suggest that IS20 treatment restores GDNF levels and neurochemical deficits in the MPTP Parkinsonian model.

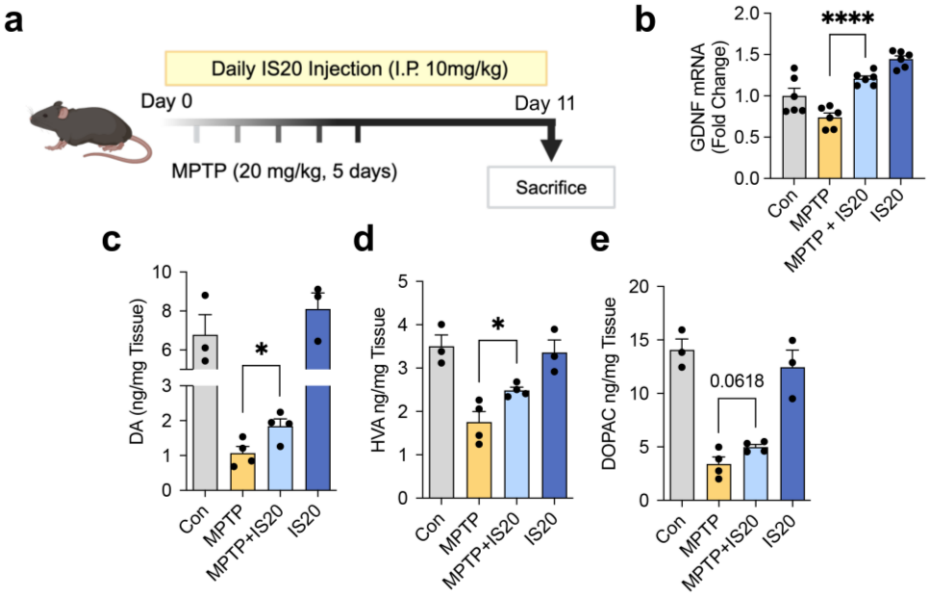


Figure 5. IS20 protects against MPTP-induced DAergic cell death in C57BL/6 mice and restores GDNF expression. (**a**) Treatment paradigm for C57BL/6 mice intraperitoneally injected with MPTP and IS20 treatments for 5 d and 12 d, respectively. Figure generated using BioRender. (**b**) RT-qPCR analysis showing GDNF gene expression in mice after 12 d of treatments with vehicle control, MPTP alone, MPTP-IS20 co-treatment, or IS20 alone. (**c**–**e**) HPLC analysis of striatal lysates from mice treated with vehicle control, MPTP alone, MPTP-IS20 co-treatment, or IS20 alone showing (**c**) DA, (**d**) homovanillic acid (HVA), and (**e**) DOPAC. Student's *t*-tests were used to evaluate MPTP vs. MPTP + IS20. * $p \leq 0.05$, **** $p < 0.0001$.

3.7. IS20 Protects Against Behavioral Deficits and DAergic Neurodegeneration in the MitoPark Mouse Model of PD

Because DAergic degeneration in the MPTP model stems from an acute neurotoxic insult and follows a rapid disease course, we next turned to the transgenic (Tg) MitoPark mouse model, which more closely recapitulates human PD's chronically progressive neurodegenerative process. This genetic model of PD was rendered by cKO of TFAM driven by the Cre/LoxP system in DAergic neurons. The subsequent mitochondrial dysfunction results in PD-like symptoms, including a steady, progressive loss of DAergic neurons over several months, with the accompanying loss of motor capacity starting at around age 12–14 wk, as well as non-motor symptoms including olfactory deficits and depression. Littermates lacking the cKO of TFAM do not exhibit deficits and serve as ideal healthy controls. In contrast to the acute MPTP model, in which i.p. administration served as a practical and reliable systemic delivery method for a short-term treatment paradigm, the chronically progressive MitoPark model required repeated long-term dosing. Therefore, IN administration was chosen as a less invasive route that provides effective brain exposure and is better suited for chronic treatment. Accordingly, we initiated a small study using MitoPark mice aged 13 wk that were randomly chosen for IN treatment with vehicle or IS20 (3 mg/kg) every other day for 4 wk (Figure 6a). Using this model allowed us to test if a more chronic IN treatment regimen attenuates the onset and progression of behavioral deficits in a slowly progressive PD context. Starting at 15 wk (14 d into treatment), vehicle-treated MitoPark mice exhibited a drastic reduction in locomotor activity (Figure 6b,c). In contrast, IS20-treated MitoPark mice exhibited modestly improved horizontal activity at this time point, and by 28 d post-treatment, their locomotor performance was significantly better than that of vehicle-treated MitoParks (Figure 6b,c). Additional behavioral analysis revealed that IS20-treated MitoPark mice had modestly but non-significantly improved motor and olfactory function as assessed by the rotarod test and social discrimination test, respectively (Supplementary Figure S4b,c). While our limited sample size prevents us from definitively establishing the behavioral outcomes of IS20 treatment, our future studies will seek to optimize the dosing schedule by employing larger-scale blinded cohort designs.

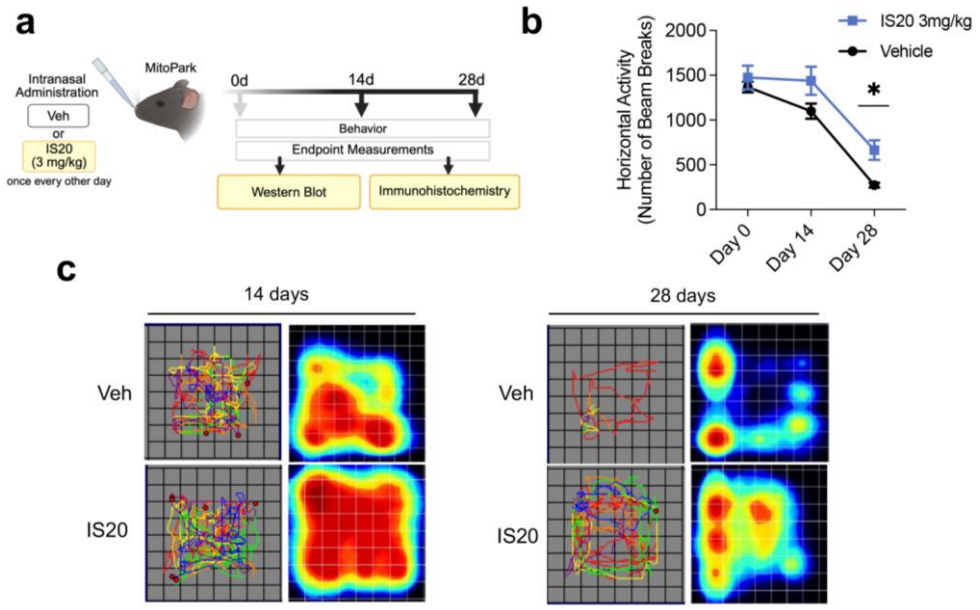


Figure 6. IS20 protects against behavioral deficits in the MitoPark model. (**a**) Treatment paradigm for MitoPark mice treated with 3 mg/kg IS20 or vehicle via intranasal administration every other day for 28 d with biweekly behavioral monitoring using VersaMax. Figure generated using BioRender. (**b**) Horizontal activity analysis of mice treated with IS20 (3 mg/kg) or vehicle after 14 and 28 d

(*n* = 2–3). (**c**) Representative track and heat plots of VersaMax analysis from 10-min activity monitoring of mice treated with IS20 (3 mg/kg) or vehicle after 14 and 28 d. The five differently colored lines in the track plot represent 2-min segments of the 10-min open-field session. * $p \leq 0.05$.

Following completion of the treatment regimen, MitoPark mice were sacrificed for tissue analysis at age 17 wk. The SN of IS20-treated MitoPark mice showed significantly increased GDNF mRNA and protein expression, as measured by RT-qPCR and Western blot, respectively, when compared to vehicle-treated mice (Figure 7a–c). TH protein levels in the MitoPark SN were also significantly protected by IS20 treatment, whereas PKR1 levels were unaffected (Figure 7b,c). Since astrocyte-derived GDNF can reduce microglia-induced neuroinflammation [55,56], we also assessed IBA1 protein levels and found a decrease in expression in the SN (Figure 7b,c), potentially indicating a reduction in microglial activation in IS20-treated mice. To confirm the functional effects of IS20-induced GDNF upregulation on DAergic neurodegeneration in MitoPark mice, brain sections from 17-wk MitoPark mice were immunostained for TH. DAB immunostaining and stereological counts of TH-positive DAergic neurons revealed significantly higher neuronal counts in the SN of IS20-treated mice compared with vehicle-treated MitoPark mice (Figure 7d). Taken together, these experiments show that IS20 IN delivery significantly protects against DAergic neuronal cell loss and mitigates behavioral deficits in the Tg MitoPark mouse model of PD.

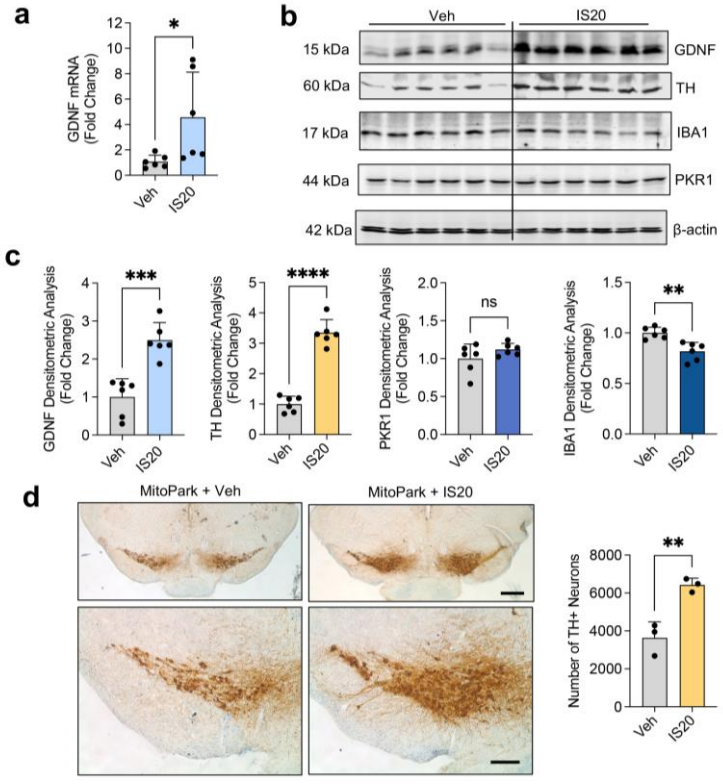


Figure 7. IS20 protects against DAergic neurodegeneration in the MitoPark model. (**a**) RT-qPCR of GDNF and of SN lysates from 13-wk-old MitoPark mice treated intranasally with IS20 (3 mg/kg) or vehicle control every other day for 28 d. (**b**) Western blot analysis probing for GDNF, TH, IBA1, and PKR1 in SN brain lysates from IS20- or vehicle-treated MitoPark mice; β-actin was used as loading control (*n* = 6). (**c**) Densitometric analysis of Western blots (shown in b) normalized to β-actin. (**d**) Tyrosine hydroxylase (TH) immunostaining of SN sections imaged at 2X (**top**) and 10X (**bottom**) magnifications with computer-assisted stereological counting of TH+ cells in the SNpc (**right**). * $p \leq 0.05$, ** $p < 0.01$, *** $p < 0.001$, **** $p < 0.0001$ when compared to vehicle control group.

3.8. IS20 Activates AKT and p44/42 MAPK Signaling Pathways and Induces Pro-Survival Bcl2 Gene Expression

Knowing that i.p. injection of IS20 activates AKT by phosphorylation in mouse hearts but not in PKR1-KO mouse hearts [39], we next explored IS20's effects on signal transduction pathways in primary mouse astrocytes. IS20 rapidly induced both AKT and p44/42 phosphorylation (Figure 8a) and promoted the expression of Bcl2 mRNA (Figure 8b). Furthermore, in C57BL/6 mice 8 h after IP injection, IS20 induced AKT phosphorylation in the striatum (Figure 8c). These experiments suggest mechanistically that IS20 promotes signaling transduction known to induce GDNF upregulation as well as other neuroprotective factors.

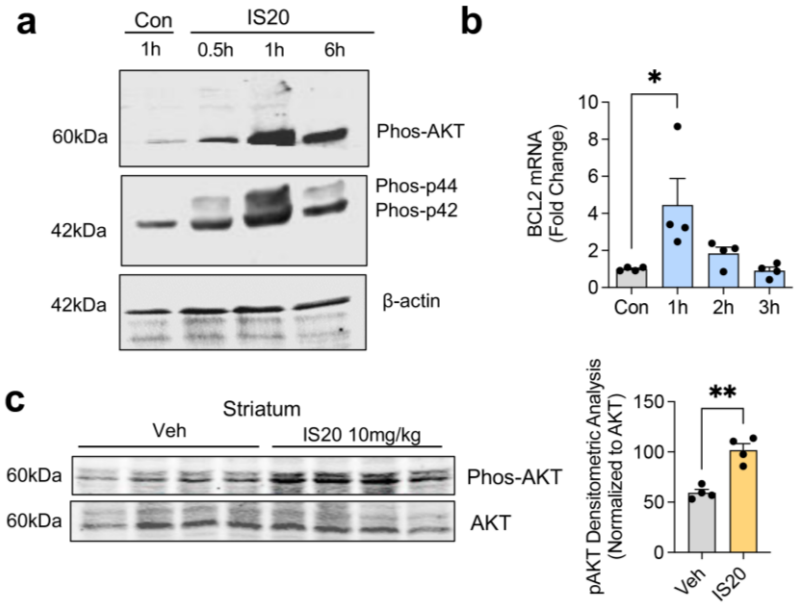


Figure 8. IS20 activates p44/42 and AKT pathways and induces pro-survival NRF2 and BCL2 gene expression. (**a**) Western blot analysis probing for phosphorylated AKT and phosphorylated p44/42 in primary mouse astrocytes treated with IS20 for 0.5–6 h. (**b**) RT-qPCR of Bcl2 gene expression in primary mouse astrocytes treated with IS20. (**c**) Western blot analysis probing for phospho-AKT and AKT in striatum lysates from C57BL/6 mice at 8 h after IP injection of IS20. * $p \leq 0.05$, ** $p < 0.01$.

4. Discussion

In this study, we demonstrated the therapeutic potential of a small-molecule PKR1 agonist, IS20, to induce GDNF expression and achieve neuroprotection in two rodent models of PD. In particular, we show that activation of PKR1 signaling through IS20 treatment rapidly stimulates GDNF gene expression and secretion in primary astrocyte and organotypic slice cultures. In our experiments with C57BL/6 mice, IN-administered IS20 successfully crossed the blood–brain barrier, reached maximum brain concentration within around 30 min, and induced robust GDNF gene expression in the nigrostriatal system as well as increased circulating GDNF levels. Using a subacute MPTP mouse model of PD, we show that IS20 protects against MPTP-induced GDNF reduction and preserves striatal DA and metabolite levels. Furthermore, we show in Tg MitoPark mice that a 4-wk course of IN-administered IS20 induced GDNF and TH levels in the SN, suppressed microglial activation, and protected against DAergic neurodegeneration. Importantly, these molecular and cellular protective effects translate to some functional improvements in locomotor activity for MitoPark mice. These findings suggest that pharmacological modulation of PK2/GDNF signaling is achievable safely and effectively through IN delivery of the PKR1 receptor agonist IS20.

PK2 activates PKR1 at an EC_{50} of 4.3 ± 1.3 nM and PKR2 at an EC_{50} of 7.3 ± 2.8 nM [57]. The similar receptor affinities suggest that the downstream effects of PK2 are largely determined by the relative expression levels of PKR1 and PKR2 on the cell surface [58]. We previously showed that PK2 signaling through PKR1 and PKR2 in neurons rapidly increases intracellular Ca^{2+} and induces phosphorylation of AKT and p44/42, leading to increases in BCL2 protein levels and mitochondrial biogenesis [36]. We also developed an efficient AAV2/5-mediated gene-delivery system, which produces robust and stable PK2 expression in the striatum and protects SN neurons from MPTP-induced neurodegeneration. In astrocytes, activation of prokineticin signaling is likely modulated by the predominant expression of PKR1 [38]. Consistent with these findings, our current study shows that the PKR1 receptor agonist IS20 rapidly increases intracellular Ca^{2+} and induces phosphorylation of AKT and p44/42 in astrocytes. Since both prokineticin and GDNF signaling depend on AKT and ERK signaling in DAergic neurons to mediate protective effects [36,53], it is therefore possible that crosstalk between prokineticin and GDNF signaling mediates IS20's pro-survival effects. Indeed, blocking AKT and p44/42 using API and PD98059, respectively, in neurons treated with PK2 protein nullifies its protective effects [36], and blocking p44/42 using PD98059 prevents GDNF release from rat glioma cells, as reported by Tanabe et al. (2012) [59]. Their findings further suggest that prokineticin and GDNF signaling converge at AKT and p44/42 in DAergic neurons to promote neuronal survival, aligning with our findings in the present study.

Previous work has demonstrated that GDNF is upregulated by ischemia [60] and that astrocyte-derived GDNF protects neuronal cultures from cell death in cases of mitochondrial damage [61]. Similarly, PK2 is upregulated by hypoxia in primary cortical culture models of ischemia [62]; it promotes endothelial cell proliferation, survival, and migration under hypoxic stress [63] and supports mitochondrial biogenesis under MPP^+-induced oxidative stress [36]. These previous findings support our hypothesis that PK2 and GDNF are co-regulated in response to metabolic and mitochondrial stress and can act in concert in the CNS and PNS. Crosstalk between PK2 and GDNF has also been described during ENS development, where both factors function as chemoattractants guiding axons during neurogenesis and neuritogenesis [33]. Moreover, PKR1 cKO causes cardiac and renal defects associated with impaired angiogenesis, reduced cell survival signaling, and defective mitochondrial and progenitor-cell functions, reinforcing the broader relevance of PK2-GDNF signaling convergence across organ systems [64].

A conclusion drawn from previous GDNF clinical trials is that although the potential for GDNF-based therapy remains high, two challenges need to be overcome: proper selection of animal-based PD models during preclinical testing and unwanted compensatory reactions or side effects associated with GDNF delivery [65]. MPTP has been the most commonly employed Parkinsonian toxicant in the generation of animal models of PD [66,67] for its ability to recapitulate features of the human disease in mice [68,69]. Although subacute MPTP treatment (3–5 daily injections) in rodents produces PD-related neuropathology, this outcome does not progress gradually, nor does it reliably reproduce the suite of behavioral deficits characterizing the human disease [70–72]. Importantly, MPTP injections leave striatal DAergic neuron projections sufficiently intact, which are then capable of retrogradely transporting GDNF to the SN [24]. Yet, recent clinical data observed in post-mortem brains of PD patients 4 years post-diagnosis revealed near-complete loss of TH-positive DAergic innervation in the caudate–putamen [73], questioning the effectiveness of delivering GDNF only in the striatum of advanced PD patients, as employed by clinical trials conducted by Amgen [74–76] and others [77,78]. Thus, the translational value of past studies relying only on acute neurodegeneration models is confounded by their intact axonal transport machinery [79]. In contrast, MitoPark mice used in the current study exhibit profound loss of striatal projections at age 17 wk, more closely

mimicking advanced PD and providing a stringent setting in which to test neuroprotective interventions. This current understanding also sheds light on earlier studies reporting that GDNF administration by intranigral injection could mitigate neuronal cell loss but did not protect against loss of terminal projections [63,80]. And by extension, intrastriatal injection of AAV-GDNF could protect against degeneration of both neuronal cell bodies and projections if administered before neuronal cell loss [81]. This is presumably because GDNF must be retrogradely transported to the neurosomata for RET signaling to mediate pro-survival effects [24]. Therefore, high GDNF expression in the striatum is less effective if GDNF's retrograde transport is disrupted due to significantly degenerated DAergic neuronal projections. In this case, increasing GDNF levels in both the striatum and SN might prove to be more effective in promoting GDNF-induced pro-survival effects [82]. Indeed, success has been achieved using AAV2-mediated neurotrophic factor gene delivery to both regions [81,83]. In our current study, IS20 induced GDNF expression levels in both the striatum and SN of MitoPark mice, potentially contributing to the protection of DAergic projections in the striatum as well as neurosomata in the SN. Although our in vitro findings demonstrate that IS20 promotes astrocytic GDNF expression, the specific cellular sources of IS20-induced GDNF upregulation in vivo remain to be determined. Together, these data indicate that performing preclinical studies in animal models that recapitulate the gradual progression of PD pathology could improve the transition from translational research to clinical trials for PD and reduce the attrition of candidate therapies.

Most current GDNF gene-delivery trials use AAV2, which has low immunogenicity and has proven safe for use in humans, but transduces predominantly neurons [84,85]. However, in the injured brain, GDNF is mainly produced by astrocytes rather than neurons [86,87], as when astrocytes secrete GDNF during ischemia as a compensatory response [88]. Astrocytes also provide the major source of GDNF in the SN of PD patients [29,30], where astrocytes and microglia outnumber neurons by ~10 to 1 [56,89]. Early studies isolated nigral GDNF from Type 1 astrocytes and found that astrocyte-derived GDNF enhances DAergic neuron survival when nigral astrocytes are co-cultured with DAergic neurons as support cell monolayers [90]. Astrocytes are also known to secrete other neurotrophic factors, such as CDNF, BDNF, and NGF. Moreover, in the gut, enteric glial cells are the major source of GDNF [91,92]. Therefore, neuroprotective efforts targeting only neurons for long-term neuronal viability are unlikely to succeed if supportive astrocytes do not provide proper neurotrophic and metabolic enrichment [93]. Indeed, several studies have found that intrastriatal, viral-mediated GDNF gene delivery causes aberrant neurite growth towards the site of application [24,41], suggesting that mimicking the endogenous mode of expression is important to achieve functional effects. Drinkut et al. (2012) [29] focused on viral delivery of GDNF into astrocytes, achieving localized, yet satisfactory neuroprotection. Building upon these studies, our findings demonstrate that pharmacological activation of PKR1 signaling enhances GDNF expression in cultured astrocytes and increases GDNF levels in the nigrostriatal system following non-invasive IS20 administration. Further cell-type-specific investigations are warranted to establish the contribution of astrocytes to IS20-induced GDNF upregulation in vivo.

The neuroprotective effects afforded by IS20 could also be mediated, in part, through the reduction of microglial activation in the SN, which has a high density of microglia [94], whose activation is affected by PD pathology [95]. Notably, the role of astrocytic GDNF appears to extend to neuroinflammation associated with neurodegeneration, as it can potently inhibit excessive production of reactive oxygen species in zymosan A-stimulated midbrain microglial cultures [56] and in LPS-stimulated primary midbrain neuron–glia cultures [96]. Thus, astrocyte-derived GDNF could mediate protective effects by its anti-inflammatory effects on activated microglia [95]. In line with previous studies, we show that IS20 treatment reduced IBA1 expression in the SN of 17-wk-old MitoPark mice. A

separate concern with GDNF-based therapies is that constitutive GDNF expression from viral transgene expression can downregulate TH expression [25], possibly due to feedback loops between GDNF and DA reuptake [97,98]. To counteract such unwanted compensatory effects, a discontinuous GDNF delivery paradigm could allow GDNF to return to basal levels [29,65]. Our pharmacodynamic studies in healthy control mice found that IS20-induced GDNF expression in the striatum and SN, as well as the whole brain, returned to basal levels 6 h post-treatment, thereby avoiding constitutive GDNF expression. Consequently, we saw increases in TH in MitoPark mice treated with IS20. While our results demonstrate that GDNF expression is induced by IS20, we cannot definitively conclude that GDNF is causally linked to the neuroprotection we observed. Future work will seek to expand our understanding of the causal signaling mechanisms underlying IS20-mediated neuroprotection.

Yet another possible cause of an unwanted compensatory effect, driven by viral transgenes in other studies [27], results from GDNF expression that is at least one or two orders of magnitude higher. In our study, we have seen 2-fold and 3-fold increases in GDNF expression induced by IS20 in the striatum and SN, respectively, and a 0.5-fold increase in GDNF expression in the whole brain relative to control levels. Furthermore, we did not see overt signs of toxicity or a significant reduction in body weight with the administered doses, routes, and study duration. This is in agreement with a previously published study, where subchronic i.p. administrations of PK2 protein, which activates PKR1 and PKR2 in a relatively non-selective fashion [99], were administered systemically in C57BL/6 mice without causing serious toxicity [100].

Despite these promising findings, several limitations warrant consideration. The relatively small sample sizes in some of our in vivo experiments and the heterogeneity of PD pathology may limit the generalizability of our findings. Challenges associated with small and heterogeneous datasets have also been highlighted in PD research [101]. Further studies involving larger cohorts and additional experimental models are warranted to validate the neuroprotective efficacy of IS20 and strengthen the translational relevance of these findings.

5. Conclusions

In summary, IS20 administration pharmacologically upregulates GDNF levels within the nigrostriatal pathway, thereby preserving DAergic neurons and their functional innervations in neuroprotective paradigms applied in PD animal models. These findings establish PK2 as a potent modulator of neurotrophic support and highlight its disease-modifying properties against dopaminergic neurodegeneration. Importantly, the favorable safety profile of IS20 underscores its translational potential, positioning it as a promising neuroprotective agent targeting GDNF signaling. Together, these results provide a strong preclinical foundation for advancing PK2 agonists into therapeutic pipelines for neuroprotection and functional restoration in PD and related neurodegenerative diseases.

Supplementary Materials: The following supporting information can be downloaded at: https://www.mdpi.com/article/10.3390/biomedicines14112521/s1, Figure S1. GDNF expression is reduced in the SN of PD patient samples and colocalizes with PKR1. (a) Double-labelling immunofluorescence for GDNF (red) and PKR1 (green) in human post-mortem nigral sections. Scale bar = 50 μm. (b) Quantitative PCR showing GDNF downregulation in striatum of PD patients. Data represented as mean ± SEM and expressed as fold-change normalized to control (n = 2–3). ** $p < 0.01$ Student's *t*-test. Figure S2. PK2 and IS20 activate PKR1 and initiate calcium mobilization. (a) AlphaFold3 modeling of PK2–PKR1 binding with PK2 in blue, the required AVITGA PK2 sequence motif in red, and PKR1 in grey. (b) IS20 complexing with PKR1. (c) Calcium assay analysis of CHO cells stably expressing PKR1 treated with 100 nM rPK2. (d) Calcium assay analysis of CHO cells

stably expressing PKR1 treated with 10 μM IS20. Figure S3. (a) Kill curve of primary mouse astrocytes treated with IS20 with corresponding EC50 measurements (right). (b) qPCR analysis of GFRa1 in primary mouse astrocytes treated with (1–10 μM IS20). (c) IS20 and IS21 molecular structures. (d) qPCR analysis of primary mouse astrocytes treated with IS20 (10 μM) or IS21 (10 μM) for 3 h. (e) Neurotrophin gene array analysis of primary mouse astrocytes treated with IS20 (10 μM). * $p < 0.05$, $p < 0.001$. Figure S4. (a) Mouse treatment paradigm (left) and liquid chromatography/mass spectrometry (LC/MS) analysis of IS20 in the brain of mice treated with IS20 (right). Figure generated using BioRender. (b) Rotarod analysis of MitoPark mice treated with IS20 (3 mg/kg) or vehicle after 28 d (n = 2–3). (c) Social discrimination analysis of MitoPark mice treated with IS20 (3 mg/kg) or vehicle, assessed in self-scent zone (left) and opposite sex zone (right) (n = 2–3).

Author Contributions: Conceptualization, J.L., A.K. and A.G.K.; Investigation, Methodology, Data Curation, Validation, Visualization, and Formal Analysis, J.L., G.C., M.N., B.N.P., M.H. and S.S.; Project Administration, Resources, Supervision, and Funding Acquisition, A.G.K., A.K., L.D., C.G.N., H.J. and V.A.; Writing—original draft, and Writing—review and editing: J.L., G.C., H.J., G.Z., A.K. and A.G.K. All authors have read and agreed to the published version of the manuscript.

Funding: This work was supported by National Institutes of Health grants R01 ES034196 and R01 NS078247. Other sources include the Johnny Isakson Endowment and the Coach Mark Richt Neurological Disease Research Fund to A.G.K. and A.K.

Institutional Review Board Statement: All animal procedures were approved by Iowa State University's Institutional Animal Care and Use Committee (IACUC), Ames, IA. Protocol number IACUC-19-188, approved 6/7/2018. For human samples, since de-identified post-mortem human brain tissues were obtained from approved national brain banks, Institutional Review Board (IRB) approval from ISU was not required.

Informed Consent Statement: Not applicable.

Data Availability Statement: The data presented in this study are available on request from the corresponding author.

Conflicts of Interest: All authors declare no actual or potential competing financial interests. A.G.K. has an equity interest in Probiome Therapeutics. The terms of this arrangement have been reviewed and approved by the University of Georgia in accordance with their conflict-of-interest policies.

Abbreviations

The following abbreviations are used in this manuscript:

GDNF	Glial cell line-derived neurotrophic factor
PD	Parkinson's disease
AAV	Adeno-associated virus
PK2	Prokineticin-2
PKR1	Prokineticin receptor 1
MPTP	1-methyl-4-phenyl-1,2,3,6-tetrahydropyridine
DAergic	Dopaminergic
L-DOPA	3,4-dihydroxy-L-phenylalanine
ENS	Enteric nervous system
CNS	Central nervous system
TH	Tyrosine hydroxylase
cKO	Conditional knockout
rGDNF	recombinant GDNF
PNS	Peripheral nervous system
OB	Olfactory bulb
IN	Intranasal
ACM	Astrocyte-conditioned media
i.p.	Intraperitoneal

LC/MS	Liquid chromatography/mass-spectrometry
GPI	Glycosylphosphatidylinositol
TFAM	Mitochondrial transcription factor A
KD	Knockdown

References

1. Barzilai, A.; Melamed, E. Molecular mechanisms of selective dopaminergic neuronal death in Parkinson's disease. *Trends Mol. Med.* **2003**, *9*, 126–132. https://doi.org/10.1016/s1471-4914(03)00020-0.
2. Jarraya, B.; Boulet, S.; Ralph, G.S.; Jan, C.; Bonvento, G.; Azzouz, M.; Miskin, J.E.; Shin, M.; Delzescaux, T.; Drouot, X.; et al. Dopamine gene therapy for Parkinson's disease in a nonhuman primate without associated dyskinesia. *Sci. Transl. Med.* **2009**, *1*, 2ra4. https://doi.org/10.1126/scitranslmed.3000130.
3. Meissner, W.G.; Frasier, M.; Gasser, T.; Goetz, C.G.; Lozano, A.; Piccini, P.; Obeso, J.A.; Rascol, O.; Schapira, A.; Voon, V.; et al. Priorities in Parkinson's disease research. *Nat. Rev. Drug Discov.* **2011**, *10*, 377–393. https://doi.org/10.1038/nrd3430.
4. Birkmayer, W.; Hornykiewicz, O. The L-3,4-dioxyphenylalanine (DOPA)-effect in Parkinson-akinesia. *Wien. Klin. Wochenschr.* **1961**, *73*, 787–788.
5. Won, S.-Y.; Park, M.-H.; You, S.-T.; Choi, S.-W.; Kim, H.-K.; McLean, C.; Bae, S.-C.; Kim, S.R.; Jin, B.K.; Lee, K.H.; et al. Nigral dopaminergic PAK4 prevents neurodegeneration in rat models of Parkinson's disease. *Sci. Transl. Med.* **2016**, *8*, 367ra170. https://doi.org/10.1126/scitranslmed.aaf1629.
6. Rascol, O.; Brooks, D.J.; Korczyn, A.D.; De Deyn, P.P.; Clarke, C.E.; Lang, A.E. A five-year study of the incidence of dyskinesia in patients with early Parkinson's disease who were treated with ropinirole or levodopa. *N. Engl. J. Med.* **2000**, *342*, 1484–1491. https://doi.org/10.1056/NEJM200005183422004.
7. Enomoto, H.; Araki, T.; Jackman, A.; Heuckeroth, R.O.; Snider, W.D.; Johnson, E.M.; Milbrandt, J. GFR alpha1-deficient mice have deficits in the enteric nervous system and kidneys. *Neuron* **1998**, *21*, 317–324. https://doi.org/10.1016/s0896-6273(00)80541-3.
8. Young, H.; Hearn, C.; Farlie, P.; Canty, A.; Thomas, P.; Newgreen, D. GDNF is a chemoattractant for enteric neural cells. *Dev. Biol.* **2001**, *229*, 503–516. https://doi.org/10.1006/dbio.2000.0100.
9. Uesaka, T.; Nagashimada, M.; Enomoto, H. GDNF signaling levels control migration and neuronal differentiation of enteric ganglion precursors. *J. Neurosci.* **2013**, *33*, 16372–16382. https://doi.org/10.1523/JNEUROSCI.2079-13.2013.
10. Pascual, A.; Hidalgo-Figueroa, M.; Piruat, J.I.; Pintado, C.O.; Gómez-Díaz, R.; López-Barneo, J. Absolute requirement of GDNF for adult catecholaminergic neuron survival. *Nat. Neurosci.* **2008**, *11*, 755–761. https://doi.org/10.1038/nn.2136.
11. Lin, L.F.; Doherty, D.H.; Lile, J.D.; Bektesh, S.; Collins, F. GDNF: A glial cell line-derived neurotrophic factor for midbrain dopaminergic neurons. *Science* **1993**, *260*, 1130–1132. https://doi.org/10.1126/science.8493557.
12. Beck, K.D.; Valverde, J.; Alexi, T.; Poulsen, K.; Moffat, B.; Vandlen, R.A.; Rosenthal, A.; Hefti, F. Mesencephalic dopaminergic neurons protected by GDNF from axotomy-induced degeneration in the adult brain. *Nature* **1995**, *373*, 339–341. https://doi.org/10.1038/373339a0.
13. Kopra, J.; Vilenius, C.; Grealish, S.; Härma, M.-A.; Varendi, K.; Lindholm, J.; Castrén, E.; Võikar, V.; Björklund, A.; Piepponen, T.P.; et al. GDNF is not required for catecholaminergic neuron survival in vivo. *Nat. Neurosci.* **2015**, *18*, 319–322. https://doi.org/10.1038/nn.3941.
14. Pascual, A.; Lopez-Barneo, J. Reply to "GDNF is not required for catecholaminergic neuron survival in vivo". *Nat. Neurosci.* **2015**, *18*, 322–323. https://doi.org/10.1038/nn.3942.
15. Bilang-Bleuel, A.; Revah, F.; Colin, P.; Locquet, I.; Robert, J.-J.; Mallet, J.; Horellou, P. Intrastriatal injection of an adenoviral vector expressing glial-cell-line-derived neurotrophic factor prevents dopaminergic neuron degeneration and behavioral impairment in a rat model of Parkinson disease. *Proc. Natl. Acad. Sci. USA* **1997**, *94*, 8818–8823. https://doi.org/10.1073/pnas.94.16.8818.
16. Bjorklund, A.; Rosenblad, C.; Winkler, C.; Kirik, D. Studies on neuroprotective and regenerative effects of GDNF in a partial lesion model of Parkinson's disease. *Neurobiol. Dis.* **1997**, *4*, 186–200. https://doi.org/10.1006/nbdi.1997.0151.
17. Kordower, J.H.; Emborg, M.E.; Bloch, J.; Ma, S.Y.; Chu, Y.; Leventhal, L.; McBride, J.; Chen, E.-Y.; Palfi, S.; Roitberg, B.Z.; et al. Neurodegeneration prevented by lentiviral vector delivery of GDNF in primate models of Parkinson's disease. *Science* **2000**, *290*, 767–773. https://doi.org/10.1126/science.290.5492.767.

18. Tseng, J.L.; Baetge, E.E.; Zurn, A.D.; Aebischer, P. GDNF reduces drug-induced rotational behavior after medial forebrain bundle transection by a mechanism not involving striatal dopamine. *J. Neurosci.* **1997**, *17*, 325–333. https://doi.org/10.1523/JNEUROSCI.17-01-00325.1997.
19. Domanskyi, A.; Saarma, M.; Airavaara, M. Prospects of Neurotrophic Factors for Parkinson's Disease: Comparison of Protein and Gene Therapy. *Hum. Gene Ther.* **2015**, *26*, 550–559. https://doi.org/10.1089/hum.2015.065.
20. Gill, S.S.; Patel, N.K.; Hotton, G.R.; O'Sullivan, K.; McCarter, R.; Bunnage, M.; Brooks, D.J.; Svendsen, C.N.; Heywood, P. Direct brain infusion of glial cell line-derived neurotrophic factor in Parkinson disease. *Nat. Med.* **2003**, *9*, 589–595. https://doi.org/10.1038/nm850.
21. Hovland, D.N.; Boyd, R.B.; Butt, M.T.; Engelhardt, J.A.; Moxness, M.S.; Ma, M.H.; Emery, M.G.; Ernst, N.B.; Reed, R.P.; Zeller, J.R.; et al. Reprint: Six-month continuous intraputamenal infusion toxicity study of recombinant methionyl human glial cell line-derived neurotrophic factor (r-metHuGDNF) in rhesus monkeys. *Toxicol. Pathol.* **2007**, *35*, 1013–1029. https://doi.org/10.1177/01926230701481899.
22. Blits, B.; Petry, H. Perspective on the Road toward Gene Therapy for Parkinson's Disease. *Front. Neuroanat.* **2017**, *10*, 128. https://doi.org/10.3389/fnana.2016.00128.
23. Remy, P. Biotherapies for Parkinson disease. *Rev. Neurol.* **2014**, *170*, 763–769. https://doi.org/10.1016/j.neurol.2014.10.002.
24. Tenenbaum, L.; Humbert-Claude, M. Glial Cell Line-Derived Neurotrophic Factor Gene Delivery in Parkinson's Disease: A Delicate Balance between Neuroprotection, Trophic Effects, and Unwanted Compensatory Mechanisms. *Front. Neuroanat.* **2017**, *11*, 29. https://doi.org/10.3389/fnana.2017.00029.
25. Tereshchenko, J.; Maddalena, A.; Bahr, M.; Kugler, S. Pharmacologically controlled, discontinuous GDNF gene therapy restores motor function in a rat model of Parkinson's disease. *Neurobiol. Dis.* **2014**, *65*, 35–42. https://doi.org/10.1016/j.nbd.2014.01.009.
26. Caumont, A.S.; Octave, J.N.; Hermans, E. Specific regulation of rat glial cell line-derived neurotrophic factor gene expression by riluzole in C6 glioma cells. *J. Neurochem.* **2006**, *97*, 128–139. https://doi.org/10.1111/j.1471-4159.2006.03711.x.
27. Ibanez, C.F.; Andressoo, J.O. Biology of GDNF and its receptors—Relevance for disorders of the central nervous system. *Neurobiol. Dis.* **2017**, *97*, 80–89. https://doi.org/10.1016/j.nbd.2016.01.021.
28. Dougherty, K.D.; Dreyfus, C.F.; Black, I.B. Brain-derived neurotrophic factor in astrocytes, oligodendrocytes, and microglia/macrophages after spinal cord injury. *Neurobiol. Dis.* **2000**, *7*, 574–585. https://doi.org/10.1006/nbdi.2000.0318.
29. Drinkut, A.; Tereshchenko, Y.; Schulz, J.B.; Bahr, M.; Kugler, S. Efficient gene therapy for Parkinson's disease using astrocytes as hosts for localized neurotrophic factor delivery. *Mol. Ther.* **2012**, *20*, 534–543. https://doi.org/10.1038/mt.2011.249.
30. Mogi, M.; Togari, A.; Kondo, T.; Mizuno, Y.; Kogure, O.; Kuno, S.; Ichinose, H.; Nagatsu, T. Glial cell line-derived neurotrophic factor in the substantia nigra from control and parkinsonian brains. *Neurosci. Lett.* **2001**, *300*, 179–181. https://doi.org/10.1016/s0304-3940(01)01577-4.
31. Laustsen, A.H.; Lomonte, B.; Lohse, B.; Fernandez, J.; Gutierrez, J.M. Unveiling the nature of black mamba (*Dendroaspis polylepis*) venom through venomics and antivenom immunoprofiling: Identification of key toxin targets for antivenom development. *J. Proteom.* **2015**, *119*, 126–142. https://doi.org/10.1016/j.jprot.2015.02.002.
32. Ngan, E.S.; Lee, K.Y.; Sit, F.Y.; Poon, H.C.; Chan, J.K.; Sham, M.H.; Lui, V.C.; Tam, P.K. Prokineticin-1 modulates proliferation and differentiation of enteric neural crest cells. *Biochim. Biophys. Acta* **2007**, *1773*, 536–545. https://doi.org/10.1016/j.bbamcr.2007.01.013.
33. Ngan, E.S.; Shum, C.K.; Poon, H.-C.; Sham, M.-H.; Garcia-Barcelo, M.-M.; Lui, V.C.; Tam, P.K. Prokineticin-1 (Prok-1) works coordinately with glial cell line-derived neurotrophic factor (GDNF) to mediate proliferation and differentiation of enteric neural crest cells. *Biochim. Biophys. Acta* **2008**, *1783*, 467–478. https://doi.org/10.1016/j.bbamcr.2007.09.005.
34. Ruiz-Ferrer, M.; Torroglosa, A.; Núñez-Torres, R.; de Agustín, J.C.; Antiñolo, G.; Borrego, S. Expression of PROKR1 and PROKR2 in human enteric neural precursor cells and identification of sequence variants suggest a role in HSCR. *PLoS ONE* **2011**, *6*, e23475. https://doi.org/10.1371/journal.pone.0023475.
35. Ng, K.L.; Li, J.-D.; Cheng, M.Y.; Leslie, F.M.; Lee, A.G.; Zhou, Q.-Y. Dependence of olfactory bulb neurogenesis on prokineticin 2 signaling. *Science* **2005**, *308*, 1923–1927. https://doi.org/10.1126/science.1112103.
36. Gordon, R.; Neal, M.L.; Luo, J.; Langley, M.R.; Harischandra, D.S.; Panicker, N.; Charli, A.; Jin, H.; Anantharam, V.; Woodruff, T.M.; et al. Prokineticin-2 upregulation during neuronal injury mediates a compensatory protective response against dopaminergic neuronal degeneration. *Nat. Commun.* **2016**, *7*, 12932. https://doi.org/10.1038/ncomms12932.
37. Neal, M.; Luo, J.; Harischandra, D.S.; Gordon, R.; Sarkar, S.; Jin, H.; Anantharam, V.; Désaubry, L.; Kanthasamy, A.; Kanthasamy, A. Prokineticin-2 promotes chemotaxis and alternative A2 reactivity of astrocytes. *Glia* **2018**, *66*, 2137–2157. https://doi.org/10.1002/glia.23467.

38. Koyama, Y.; Kiyo-Oka, M.; Osakada, M.; Horiguchi, N.; Shintani, N.; Ago, Y.; Kakuda, M.; Baba, A.; Matsuda, T. Expression of prokineticin receptors in mouse cultured astrocytes and involvement in cell proliferation. *Brain Res.* **2006**, *1112*, 65–69. https://doi.org/10.1016/j.brainres.2006.07.013.
39. Gasser, A.; Brogi, S.; Urayama, K.; Nishi, T.; Kurose, H.; Tafi, A.; Ribeiro, N.; Désaubry, L.; Nebigil, C.G. Discovery and cardioprotective effects of the first non-Peptide agonists of the G protein-coupled prokineticin receptor-1. *PLoS ONE* **2015**, *10*, e0121027. https://doi.org/10.1371/journal.pone.0121027.
40. Georgievska, B.; Kirik, D.; Bjorklund, A. Overexpression of glial cell line-derived neurotrophic factor using a lentiviral vector induces time- and dose-dependent downregulation of tyrosine hydroxylase in the intact nigrostriatal dopamine system. *J. Neurosci.* **2004**, *24*, 6437–6445. https://doi.org/10.1523/JNEUROSCI.1122-04.2004.
41. Georgievska, B.; Kirik, D.; Bjorklund, A. Aberrant sprouting and downregulation of tyrosine hydroxylase in lesioned nigrostriatal dopamine neurons induced by long-lasting overexpression of glial cell line derived neurotrophic factor in the striatum by lentiviral gene transfer. *Exp. Neurol.* **2002**, *177*, 461–474. https://doi.org/10.1006/exnr.2002.8006.
42. Sajadi, A.; Bauer, M.; Thony, B.; Aebischer, P. Long-term glial cell line-derived neurotrophic factor overexpression in the intact nigrostriatal system in rats leads to a decrease of dopamine and increase of tetrahydrobiopterin production. *J. Neurochem.* **2005**, *93*, 1482–1486. https://doi.org/10.1111/j.1471-4159.2005.03139.x.
43. Bargues-Carot, A.; Kondru, N.; Haller, M.; Zenitsky, G.; Jin, H.; Anantharam, V.; Kanthasamy, A.; Kanthasamy, A.G. Neurotoxic Effect of Manganese and Vanadium Co-Exposure in Animal Models of Parkinson's Disease. *Int. J. Mol. Sci.* **2026**, *27*, 1757. https://doi.org/10.3390/ijms27041757.
44. Langley, M.R.; Ghaisas, S.; Ay, M.; Luo, J.; Palanisamy, B.N.; Jin, H.; Anantharam, V.; Kanthasamy, A.; Kanthasamy, A.G. Manganese exposure exacerbates progressive motor deficits and neurodegeneration in the MitoPark mouse model of Parkinson's disease: Relevance to gene and environment interactions in metal neurotoxicity. *Neurotoxicology* **2018**, *64*, 240–255. https://doi.org/10.1016/j.neuro.2017.06.002.
45. Padhi, P.; Abdalla, A.; Schneider, B.; Backes, N.; Otto, A.A.; Scheibe, I.J.; Thomas, J.P.; Khadse, G.; Samidurai, M.; Jochmans, A.K.; et al. Bioengineered gut bacterium synthesizing levodopa alleviates motor deficits in models of Parkinson's disease. *Cell Host Microbe* **2025**, *33*, 1837–1854 e1813. https://doi.org/10.1016/j.chom.2025.10.005.
46. Sarkar, S.; Nguyen, H.M.; Malovic, E.; Luo, J.; Langley, M.; Palanisamy, B.N.; Singh, N.; Manne, S.; Neal, M.; Gabrielle, M.; et al. Kv1.3 modulates neuroinflammation and neurodegeneration in Parkinson's disease. *J. Clin. Investig.* **2020**, *130*, 4195–4212. https://doi.org/10.1172/JCI136174.
47. Chauhan, N.B.; Siegel, G.J.; Lee, J.M. Depletion of glial cell line-derived neurotrophic factor in substantia nigra neurons of Parkinson's disease brain. *J. Chem. Neuroanat.* **2001**, *21*, 277–288. https://doi.org/10.1016/s0891-0618(01)00115-6.
48. Hunot, S.; Bernard, V.; Faucheux, B.; Leguern, E.; Brana, C.; Gautris, P.P.; Bloch, B.; Agid, Y.; Hirsch, E.C.; Boissière, F.; et al. Glial cell line-derived neurotrophic factor (GDNF) gene expression in the human brain: A post mortem in situ hybridization study with special reference to Parkinson's disease. *J. Neural Transm.* **1996**, *103*, 1043–1052. https://doi.org/10.1007/BF01291789.
49. Gasser, A.; Chen, Y.-W.; Audebrand, A.; Daglayan, A.; Charavin, M.; Escoubet, B.; Karpov, P.; Tetko, I.; Chan, M.W.; Cardinale, D.; et al. Prokineticin Receptor-1 Signaling Inhibits Dose- and Time-Dependent Anthracycline-Induced Cardiovascular Toxicity Via Myocardial and Vascular Protection. *JACC Cardio Oncol.* **2019**, *1*, 84–102. https://doi.org/10.1016/j.jaccao.2019.06.003.
50. Ngan, E.S.; Tam, P.K. Prokineticin-signaling pathway. *Int. J. Biochem. Cell Biol.* **2008**, *40*, 1679–1684. https://doi.org/10.1016/j.biocel.2008.03.010.
51. Lochhead, J.J.; Thorne, R.G. Intranasal delivery of biologics to the central nervous system. *Adv. Drug Deliv. Rev.* **2012**, *64*, 614–628. https://doi.org/10.1016/j.addr.2011.11.002.
52. Hernando, S.; Herran, E.; Figueiro-Silva, J.; Pedraz, J.L.; Igartua, M.; Carro, E.; Hernandez, R.M. Intranasal Administration of TAT-Conjugated Lipid Nanocarriers Loading GDNF for Parkinson's Disease. *Mol. Neurobiol.* **2018**, *55*, 145–155. https://doi.org/10.1007/s12035-017-0728-7.
53. Sariola, H.; Saarma, M. Novel functions and signalling pathways for GDNF. *J. Cell Sci.* **2003**, *116*, 3855–3862. https://doi.org/10.1242/jcs.00786.
54. Wang, Y.; Lin, S.Z.; Chiou, A.L.; Williams, L.R.; Hoffer, B.J. Glial cell line-derived neurotrophic factor protects against ischemia-induced injury in the cerebral cortex. *J. Neurosci.* **1997**, *17*, 4341–4348. https://doi.org/10.1523/JNEUROSCI.17-11-04341.1997.
55. Chen, S.-H.; Oyarzabal, E.A.; Sung, Y.-F.; Chu, C.-H.; Wang, Q.; Chen, S.-L.; Lu, R.-B.; Hong, J.-S. Microglial regulation of immunological and neuroprotective functions of astroglia. *Glia* **2015**, *63*, 118–131. https://doi.org/10.1002/glia.22738.
56. Rocha, S.M.; Cristovao, A.C.; Campos, F.L.; Fonseca, C.P.; Baltazar, G. Astrocyte-derived GDNF is a potent inhibitor of microglial activation. *Neurobiol. Dis.* **2012**, *47*, 407–415. https://doi.org/10.1016/j.nbd.2012.04.014.

57. Lin, D.C.-H.; Bullock, C.M.; Ehlert, F.J.; Chen, J.-L.; Tian, H.; Zhou, Q.-Y. Identification and molecular characterization of two closely related G protein-coupled receptors activated by prokineticins/endocrine gland vascular endothelial growth factor. *J. Biol. Chem.* **2002**, *277*, 19276–19280. https://doi.org/10.1074/jbc.M202139200.
58. Attramadal, H. Prokineticins and the heart: Diverging actions elicited by signalling through prokineticin receptor-1 or -2. *Cardiovasc. Res.* **2009**, *81*, 3–4. https://doi.org/10.1093/cvr/cvn306.
59. Tanabe, K.; Matsushima-Nishiwaki, R.; Iida, M.; Kozawa, O.; Iida, H. Involvement of phosphatidylinositol 3-kinase/Akt on basic fibroblast growth factor-induced glial cell line-derived neurotrophic factor release from rat glioma cells. *Brain Res.* **2012**, *1463*, 21–29. https://doi.org/10.1016/j.brainres.2012.04.057.
60. Yamagata, K.; Tagami, M.; Ikeda, K.; Tsumagari, S.; Yamori, Y.; Nara, Y. Differential regulation of glial cell line-derived neurotrophic factor (GDNF) mRNA expression during hypoxia and reoxygenation in astrocytes isolated from stroke-prone spontaneously hypertensive rats. *Glia* **2002**, *37*, 1–7. https://doi.org/10.1002/glia.10003.
61. Lin, C.-H.; Cheng, F.-C.; Lu, Y.-Z.; Chu, L.-F.; Wang, C.-H.; Hsueh, C.-M. Protection of ischemic brain cells is dependent on astrocyte-derived growth factors and their receptors. *Exp. Neurol.* **2006**, *201*, 225–233. https://doi.org/10.1016/j.expneurol.2006.04.014.
62. Cheng, M.Y.; Lee, A.G.; Culbertson, C.; Sun, G.; Talati, R.K.; Manley, N.C.; Li, X.; Zhao, H.; Lyons, D.M.; Zhou, Q.-Y.; et al. Prokineticin 2 is an endangering mediator of cerebral ischemic injury. *Proc. Natl. Acad. Sci. USA* **2012**, *109*, 5475–5480. https://doi.org/10.1073/pnas.1113363109.
63. LeCouter, J.; Lin, R.; Tejada, M.; Frantz, G.; Peale, F.; Hillan, K.J.; Ferrara, N. The endocrine-gland-derived VEGF homologue Bv8 promotes angiogenesis in the testis: Localization of Bv8 receptors to endothelial cells. *Proc. Natl. Acad. Sci. USA* **2003**, *100*, 2685–2690. https://doi.org/10.1073/pnas.0337667100.
64. Boulberdaa, M.; Turkeri, G.; Urayama, K.; Dormishian, M.; Szatkowski, C.; Zimmer, L.; Messaddeq, N.; Laugel, V.; Dollé, P.; Nebigil, C.G. Genetic inactivation of prokineticin receptor-1 leads to heart and kidney disorders. *Arterioscler. Thromb. Vasc. Biol.* **2011**, *31*, 842–850. https://doi.org/10.1161/ATVBAHA.110.222323.
65. Taylor, H.; Barua, N.; Bienemann, A.; Wyatt, M.; Castrique, E.; Foster, R.; Luz, M.; Fibiger, C.; Mohr, E.; Gill, S. Clearance and toxicity of recombinant methionyl human glial cell line-derived neurotrophic factor (r-metHu GDNF) following acute convection-enhanced delivery into the striatum. *PLoS ONE* **2013**, *8*, e56186. https://doi.org/10.1371/journal.pone.0056186.
66. Beal, M.F. Experimental models of Parkinson's disease. *Nat. Rev. Neurosci.* **2001**, *2*, 325–334. https://doi.org/10.1038/35072550.
67. Przedborski, S.; Jackson-Lewis, V.; Naini, A.B.; Jakowec, M.; Petzinger, G.; Miller, R.; Akram, M. The parkinsonian toxin 1-methyl-4-phenyl-1,2,3,6-tetrahydropyridine (MPTP): A technical review of its utility and safety. *J. Neurochem.* **2001**, *76*, 1265–1274. https://doi.org/10.1046/j.1471-4159.2001.00183.x.
68. Davis, G.C.; Williams, A.C.; Markey, S.P.; Ebert, M.H.; Caine, E.D.; Reichert, C.M.; Kopin, I.J. Chronic Parkinsonism secondary to intravenous injection of meperidine analogues. *Psychiatry Res.* **1979**, *1*, 249–254. https://doi.org/10.1016/0165-1781(79)90006-4.
69. Langston, J.W.; Ballard, P.; Tetrud, J.W.; Irwin, I. Chronic Parkinsonism in humans due to a product of meperidine-analog synthesis. *Science* **1983**, *219*, 979–980. https://doi.org/10.1126/science.6823561.
70. Rommelfanger, K.S.; Edwards, G.L.; Freeman, K.G.; Liles, L.C.; Miller, G.W.; Weinshenker, D. Norepinephrine loss produces more profound motor deficits than MPTP treatment in mice. *Proc. Natl. Acad. Sci. USA* **2007**, *104*, 13804–13809. https://doi.org/10.1073/pnas.0702753104.
71. Schober, A. Classic toxin-induced animal models of Parkinson's disease: 6-OHDA and MPTP. *Cell Tissue Res.* **2004**, *318*, 215–224. https://doi.org/10.1007/s00441-004-0938-y.
72. Tillerson, J.L.; Caudle, W.M.; Reveron, M.E.; Miller, G.W. Detection of behavioral impairments correlated to neurochemical deficits in mice treated with moderate doses of 1-methyl-4-phenyl-1,2,3,6-tetrahydropyridine. *Exp. Neurol.* **2002**, *178*, 80–90. https://doi.org/10.1006/exnr.2002.8021.
73. Kordower, J.H.; Olanow, C.W.; Dodiya, H.B.; Chu, Y.; Beach, T.G.; Adler, C.H.; Halliday, G.M.; Bartus, R.T. Disease duration and the integrity of the nigrostriatal system in Parkinson's disease. *Brain* **2013**, *136*, 2419–2431. https://doi.org/10.1093/brain/awt192.
74. Lang, A.E.; Gill, S.; Patel, N.K.; Lozano, A.; Nutt, J.G.; Penn, R.; Brooks, D.J.; Hotton, G.; Moro, E.; Heywood, P.; et al. Randomized controlled trial of intraputamenal glial cell line-derived neurotrophic factor infusion in Parkinson disease. *Ann. Neurol.* **2006**, *59*, 459–466. https://doi.org/10.1002/ana.20737.
75. Nutt, J.; Burchiel, K.; Comella, C.; Jankovic, J.; Lang, A.; Laws, E.; Lozano, A.; Penn, R.; Simpson, R.; Stacy, M.; et al. Randomized, double-blind trial of glial cell line-derived neurotrophic factor (GDNF) in PD. *Neurology* **2003**, *60*, 69–73. https://doi.org/10.1212/wnl.60.1.69.

76. Tatarewicz, S.M.; Wei, X.; Gupta, S.; Masterman, D.; Swanson, S.J.; Moxness, M.S. Development of a maturing T-cell-mediated immune response in patients with idiopathic Parkinson's disease receiving r-metHuGDNF via continuous intraputaminal infusion. *J. Clin. Immunol.* **2007**, *27*, 620–627. https://doi.org/10.1007/s10875-007-9117-8.
77. Slevin, J.T.; Gerhardt, G.A.; Smith, C.D.; Gash, D.M.; Kryscio, R.; Young, B. Improvement of bilateral motor functions in patients with Parkinson disease through the unilateral intraputaminal infusion of glial cell line-derived neurotrophic factor. *J. Neurosurg.* **2005**, *102*, 216–222. https://doi.org/10.3171/jns.2005.102.2.0216.
78. Slevin, J.T.; Gash, D.M.; Smith, C.D.; Gerhardt, G.A.; Kryscio, R.; Chebrolu, H.; Walton, A.; Wagner, R.; Young, A.B. Unilateral intraputamenal glial cell line-derived neurotrophic factor in patients with Parkinson disease: Response to 1 year of treatment and 1 year of withdrawal. *J. Neurosurg.* **2007**, *106*, 614–620. https://doi.org/10.3171/jns.2007.106.4.614.
79. Herzog, C.D.; Brown, L.; Kruegel, B.R.; Wilson, A.; Tansey, M.G.; Gage, F.H.; Johnson, E.M.; Bartus, R.T. Enhanced neurotrophic distribution, cell signaling and neuroprotection following substantia nigral versus striatal delivery of AAV2-NRTN (CERE-120). *Neurobiol. Dis.* **2013**, *58*, 38–48. https://doi.org/10.1016/j.nbd.2013.04.011.
80. Mandel, R.J.; Spratt, S.K.; Snyder, R.O.; Leff, S.E. Midbrain injection of recombinant adeno-associated virus encoding rat glial cell line-derived neurotrophic factor protects nigral neurons in a progressive 6-hydroxydopamine-induced degeneration model of Parkinson's disease in rats. *Proc. Natl. Acad. Sci. USA* **1997**, *94*, 14083–14088. https://doi.org/10.1073/pnas.94.25.14083.
81. Kirik, D.; Rosenblad, C.; Bjorklund, A.; Mandel, R.J. Long-term rAAV-mediated gene transfer of GDNF in the rat Parkinson's model: Intrastriatal but not intranigral transduction promotes functional regeneration in the lesioned nigrostriatal system. *J. Neurosci.* **2000**, *20*, 4686–4700. https://doi.org/10.1523/JNEUROSCI.20-12-04686.2000.
82. Marks, W.J.; Bartus, R.T.; Siffert, J.; Davis, C.S.; Lozano, A.; Boulis, N.; Vitek, J.; Stacy, M.; Turner, D.; Verhagen, L.; et al. Gene delivery of AAV2-neurturin for Parkinson's disease: A double-blind, randomised, controlled trial. *Lancet Neurol.* **2010**, *9*, 1164–1172. https://doi.org/10.1016/S1474-4422(10)70254-4.
83. Kordower, J.H.; Herzog, C.D.; Dass, B.; Bakay, R.A.E.; Stansell, J.; Gasmi, M.; Bartus, R.T. Delivery of neurturin by AAV2 (CERE-120)-mediated gene transfer provides structural and functional neuroprotection and neurorestoration in MPTP-treated monkeys. *Ann. Neurol.* **2006**, *60*, 706–715. https://doi.org/10.1002/ana.21032.
84. Ruitenberg, M.J.; Eggers, R.; Boer, G.J.; Verhaagen, J. Adeno-associated viral vectors as agents for gene delivery: Application in disorders and trauma of the central nervous system. *Methods* **2002**, *28*, 182–194. https://doi.org/10.1016/s1046-2023(02)00222-0.
85. Towne, C.; Pertin, M.; Beggah, A.T.; Aebischer, P.; Decosterd, I. Recombinant adeno-associated virus serotype 6 (rAAV2/6)-mediated gene transfer to nociceptive neurons through different routes of delivery. *Mol. Pain.* **2009**, *5*, 52. https://doi.org/10.1186/1744-8069-5-52.
86. Bresjanac, M.; Antauer, G. Reactive astrocytes of the quinolinic acid-lesioned rat striatum express GFRalpha1 as well as GDNF in vivo. *Exp. Neurol.* **2000**, *164*, 53–59. https://doi.org/10.1006/exnr.2000.7416.
87. Nakagawa, T.; Schwartz, J.P. Gene expression profiles of reactive astrocytes in dopamine-depleted striatum. *Brain Pathol.* **2004**, *14*, 275–280. https://doi.org/10.1111/j.1750-3639.2004.tb00064.x.
88. Yamagata, K.; Hakata, K.; Maeda, A.; Mochizuki, C.; Matsufuji, H.; Chino, M.; Yamori, Y. Adenosine induces expression of glial cell line-derived neurotrophic factor (GDNF) in primary rat astrocytes. *Neurosci. Res.* **2007**, *59*, 467–474. https://doi.org/10.1016/j.neures.2007.08.016.
89. Azevedo, F.A.C.; Carvalho, L.R.B.; Grinberg, L.T.; Farfel, J.M.; Ferretti, R.E.L.; Leite, R.E.P.; Filho, W.J.; Lent, R.; Herculano-Houzel, S. Equal numbers of neuronal and nonneuronal cells make the human brain an isometrically scaled-up primate brain. *J. Comp. Neurol.* **2009**, *513*, 532–541. https://doi.org/10.1002/cne.21974.
90. O'Malley, E.K.; Sieber, B.A.; Black, I.B.; Dreyfus, C.F. Mesencephalic type I astrocytes mediate the survival of substantia nigra dopaminergic neurons in culture. *Brain Res.* **1992**, *582*, 65–70. https://doi.org/10.1016/0006-8993(92)90317-3.
91. von Boyen, G.B.; Schulte, N.; Pflüger, C.; Spaniol, U.; Hartmann, C.; Steinkamp, M. Distribution of enteric glia and GDNF during gut inflammation. *BMC Gastroenterol.* **2011**, *11*, 3. https://doi.org/10.1186/1471-230X-11-3.
92. Steinkamp, M.; Gundel, H.; Schulte, N.; Spaniol, U.; Pflueger, C.; Zizer, E.; von Boyen, G.B. GDNF protects enteric glia from apoptosis: Evidence for an autocrine loop. *BMC Gastroenterol.* **2012**, *12*, 6. https://doi.org/10.1186/1471-230X-12-6.
93. Takano, T.; Oberheim, N.; Cotrina, M.L.; Nedergaard, M. Astrocytes and ischemic injury. *Stroke* **2009**, *40*, S8–S12. https://doi.org/10.1161/STROKEAHA.108.533166.
94. Ouchi, Y.; Yoshikawa, E.; Sekine, Y.; Futatsubashi, M.; Kanno, T.; Ogusu, T.; Torizuka, T. Microglial activation and dopamine terminal loss in early Parkinson's disease. *Ann. Neurol.* **2005**, *57*, 168–175. https://doi.org/10.1002/ana.20338.

95. Rickert, U.; Grampp, S.; Wilms, H.; Spreu, J.; Knerlich-Lukoschus, F.; Held- Feindt, J.; Lucius, R. Glial Cell Line-Derived Neurotrophic Factor Family Members Reduce Microglial Activation via Inhibiting p38MAPKs-Mediated Inflammatory Responses. *J. Neurodegener. Dis.* **2014**, *2014*, 369468. https://doi.org/10.1155/2014/369468.
96. Wu, H.-M.; Tzeng, N.-S.; Qian, L.; Wei, S.-J.; Hu, X.; Chen, S.-H.; Rawls, S.M.; Flood, P.; Hong, J.-S.; Lu, R.-B. Novel neuroprotective mechanisms of memantine: Increase in neurotrophic factor release from astroglia and anti-inflammation by preventing microglial activation. *Neuropsychopharmacology* **2009**, *34*, 2344–2357. https://doi.org/10.1038/npp.2009.64.
97. Gomes, C.A.; Vaz, S.H.; Ribeiro, J.A.; Sebastiao, A.M. Glial cell line-derived neurotrophic factor (GDNF) enhances dopamine release from striatal nerve endings in an adenosine A2A receptor-dependent manner. *Brain Res.* **2006**, *1113*, 129–136. https://doi.org/10.1016/j.brainres.2006.07.025.
98. Kopra, J.J.; Panhelainen, A.; Bjerkén, S.A.; Porokuokka, L.L.; Varendi, K.; Olfat, S.; Montonen, H.; Piepponen, T.P.; Saarma, M.; Andressoo, J.-O. Dampened Amphetamine-Stimulated Behavior and Altered Dopamine Transporter Function in the Absence of Brain GDNF. *J. Neurosci.* **2017**, *37*, 1581–1590. https://doi.org/10.1523/JNEUROSCI.1673-16.2016.
99. Lattanzi, R.; Sacerdote, P.; Franchi, S.; Canestrelli, M.; Miele, R.; Barra, D.; Visentin, S.; DeNuccio, C.; Porreca, F.; De Felice, M.; et al. Pharmacological activity of a Bv8 analogue modified in position 24. *Br. J. Pharmacol.* **2012**, *166*, 950–963. https://doi.org/10.1111/j.1476-5381.2011.01797.x.
100. Beale, K.; Gardiner, J.; Bewick, G.; Hostomska, K.; Patel, N.; Hussain, S.; Jayasena, C.; Ebling, F.; Jethwa, P.; Prosser, H.; et al. Peripheral administration of prokineticin 2 potently reduces food intake and body weight in mice via the brainstem. *Br. J. Pharmacol.* **2013**, *168*, 403–410. https://doi.org/10.1111/j.1476-5381.2012.02191.x.
101. Zhao, H.; Xie, J.; Lei, Y.; Cao, H.; Cao, J.; Liao, W.-H. Federated Transferring Multi-Channel CNN for Diagnosis of Parkinson's Disease under Unseen and Small Data. *IEEE J. Biomed. Health Inform.* **2025**, 1–12. https://doi.org/10.1109/JBHI.2025.3605772.

Disclaimer/Publisher's Note: The statements, opinions and data contained in all publications are solely those of the individual author(s) and contributor(s) and not of MDPI and/or the editor(s). MDPI and/or the editor(s) disclaim responsibility for any injury to people or property resulting from any ideas, methods, instructions or products referred to in the content.